Environmental Modelling and Software 133 (2020) 104818

Contents lists available at ScienceDirect

Environmental Modelling and Software

journal homepage: http://www.elsevier.com/locate/envsoft

Evaluating the 10% wind speed rule of thumb for estimating a wildfire's forward rate of spread against an extensive independent set of observations

Miguel G. Cruz [a,*], Martin E. Alexander [b], Paulo M. Fernandes [c,d], Musa Kilinc [e], Ângelo Sil [c,f]

[a] CSIRO, GPO Box 1700, Canberra, ACT, 2601, Australia
[b] Wild Rose Fire Behaviour, 180 - 50434 Range Road 232, Leduc County, AB, T4X 0L1, Canada
[c] Centro de Investigação e de Tecnologias Agroambientais e Biológicas, Universidade de Trás-os-Montes e Alto Douro, Quinta de Prados, 5000-801 Vila Real, Portugal
[d] ForestWISE - Collaborative Laboratory for Integrated Forest and Fire Management, Quinta de Prados, 5000-801 Vila Real, Portugal
[e] Country Fire Authority, Fire and Emergency Management, PO Box 701, Mt Waverley, VIC, 3149, Australia
[f] Centro de Investigação Em Biodiversidade e Recursos Genéticos, Campus Agrário de Vairão, Rua Padre Armando Quintas, N° 7, 4485-661 Vairão, Portugal

ARTICLE INFO

Keywords:
Crown fire
Fine dead fuel moisture content
Fire behaviour
Fire prediction
Fire propagation
Fire weather
Fuel type
Model error

ABSTRACT

The prediction of wildfire rate of spread and growth under high wind speeds and dry fuel moisture conditions is key to taking proactive actions to warn and in turn protect communities. We used two datasets of wildfires spreading under critical fire weather conditions to evaluate an existing rule of thumb that equates the forward rate of fire spread to 10% of the average open wind speed. The rule predicted the observed rates of fire spread with an overall mean absolute error of 1.7 km h^{-1}. The absolute error magnitude was consistent across the range in observed rates of fire spread, resulting in a reduction in percent error with an increase in spread rates. Mean absolute percent errors close to 20% were obtained for wildfires spreading faster than 2.0 km h^{-1}. The implications of model errors in the forecasting of fire spread with respect to community warning and safety are discussed.

1. Introduction

Early and contemporaneous research into the effects of global warming on wildfire activity have forecasted an increase in the length of the fire seasons and the number of days of extreme fire danger when large fire spread events can occur (e.g. Ryan, 1991; Beer and Williams, 1995; Barbero et al., 2020). The events of the last two decades or so have corroborated these hypotheses, with an increase in the number of highly destructive wildfires globally (Tedim et al., 2020). Associated with many of these events is the substantial loss of human life and property at unprecedented rates (Teague et al., 2010; Goldammer et al., 2019; Gee and Anguiano, 2020).

Despite the science of fire behaviour prediction being well established in many parts of the globe (Scott et al., 2014), it is clear, that even in countries with a notable investment in fire behaviour research and operational fire intelligence (e.g. situational awareness, fire spread forecasting, etc.), fires can still surprise fire management and emergency response agencies and cause a large number of fatalities. This is largely due to a combination of factors, including the inability of these agencies to forecast a wildfire's propagation, rapidly and effectively communicate the potential wildfire threat to the public and take the necessary actions to safeguard human lives.

Wildfires driven by strong winds (Fig. 1a–c) that within a few hours of their ignition grow to a large size and quickly impact communities with little or no official warning are often associated with multiple fatalities (Cruz et al., 2012; Blanchi et al., 2014; Brewer and Clements, 2019; Xanthopoulos and Athanasiou, 2019). For this type of fires, many of the methods used by specialised fire behaviour analysts (Scott et al., 2014; Neale and May 2018) imbedded in incident management teams or coordination centres to generate fire spread predictions (Andrews et al., 2007; Giannaros et al., 2019; Neale and May 2020), might well fail to meet the necessary urgency associated with such events.

Cruz and Alexander (2019) developed a rule of thumb for obtaining a first approximation of a wildfire's forward rate of spread in conifer forests, eucalypt forests, and shrublands but not in grasslands. The rule of thumb states that a wildfire rate of forward spread is approximately 10% of the average 10-m open wind speed. The rule was found to be most appropriate for strong wind and dry fuel conditions (i.e. both fine fuel moisture and overall long-term landscape dryness) associated with fast-spreading wildfires, where one would consider that "time is of the

* Corresponding author.
E-mail address: miguel.cruz@csiro.au (M.G. Cruz).

https://doi.org/10.1016/j.envsoft.2020.104818
Received 25 June 2020; Received in revised form 27 July 2020; Accepted 30 July 2020
Available online 17 August 2020

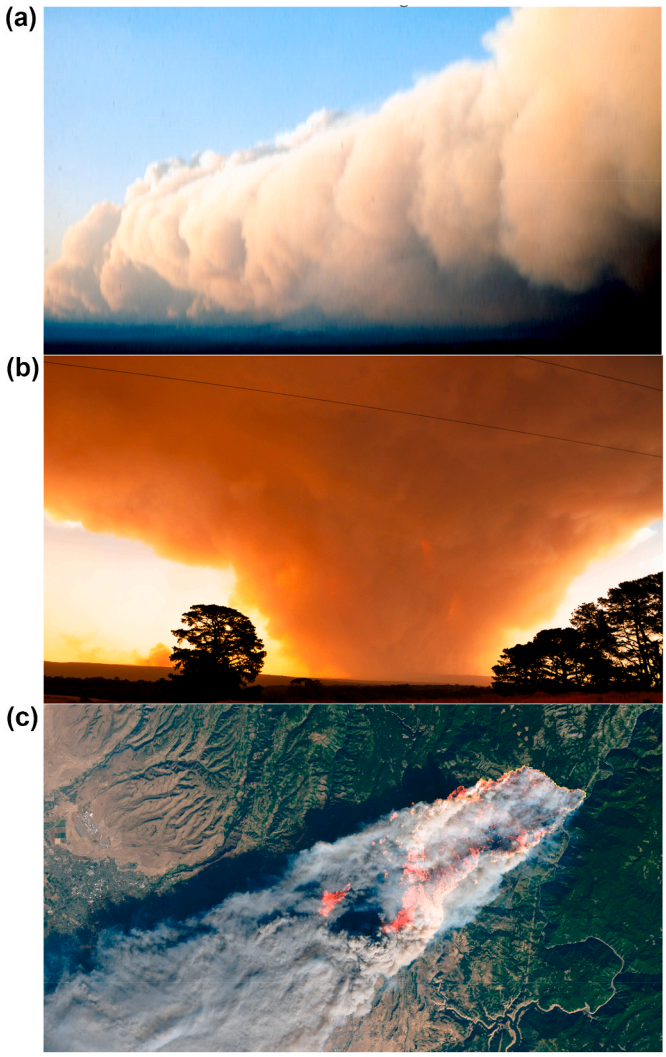

Fig. 1. View of the convection plumes or columns of three fast-spreading wildfires: (a) the Canyon Creek fire in Montana, USA, at approximately 19:00–20:00 during its main 34-km run on September 6, 1988 (photo by James Dolan, USFS); (b) under the plume of the Kilmore East fire in Victoria, Australia, at approximately 16:00 on February 7, 2009 (CSIRO file image); and (c) Landsat 8 image of the Camp fire in northern California, USA, at 10:45 on November 9, 2018, as it was burning through the town of Paradise (image by Joshua Stevens, NASA).

essence" for public warnings and evacuation notices.

The rule of thumb was considered to be appropriate for wildfires spreading over level to gently undulating topography and in cases where large wildfires advance across drainages with alternating upslope and downslope runs. Under extended drought conditions, fuels in mountainous topography are readily able to burn regardless of the variations in terrain characteristics (Cheney, 1981), When winds are suitably strong and accordingly sustained, a high intensity wildfire can continue to spread for several hours, burning out entire forested drainages and crossing mountain ridges that would normally be a barrier to fire growth (Rothermel, 1991). One such spectacular event occurred on September 6, 1988, when the Canyon Creek fire, under the influence of a dry cold front, advanced eastward across the Continental Divide (Fig. 1a) and out onto the plains of west-central Montana, USA (Goens, 1990).

Although the empirical basis of the rule of thumb makes it a reflection of the broad wildfire dataset used in its development, no independent evaluation of its performance has been carried out up to now. Here we examine the robustness of this rule of thumb by evaluating its predictive ability against independent wildfire datasets.

2. Methods

Observations of forward rate of fire spread were compiled from two different databases. This included that of Harris et al. (2011) and Kilinc et al. (2012) for Southern Australia wildfires and the BONFIRE global fire behaviour database (Fernandes et al., 2020).

The dataset extracted from Harris et al. (2011) and Kilinc et al. (2012) was limited to wildfires in eucalypt forests (Luke and McArthur, 1978) and included detailed information on fire size, fuel characteristics and predictions from rate of fire spread models currently used in South-eastern Australia (McArthur, 1967; Cheney et al., 2012). The dataset extracted from BONFIRE is broader, containing data from wildfires in shrublands, eucalypt forests and conifer forests, but overall less detailed regarding fire size and fuel characteristics.

2.1. Southern Australia database

Kilinc et al. (2012) assembled a fire behaviour database of Australian wildfires occurring in native eucalypt forests. This dataset is largely based on the data collated by Harris et al. (2011) aimed at evaluating the effects of fire weather and fire behaviour on community impacts, although some new fires were added to the database by Kilinc et al. (2012). The combined dataset from Harris et al. (2011) and Kilinc et al. (2012) used in the current study is given in Table A1 of the Appendix.

2.1.1. Fire spread isochrones and forward rate of fire spread

Spatial fire propagation data, including isochrones of progression at given time intervals, were derived from published (e.g. CFA, 1999) and unpublished wildfire case studies, reports, aerial imagery (photography and infra-red line scans), and newspaper articles. Many of the documented wildfires occurred prior to the 1980s, with information regarding the spatial attributes of these fires recorded in the form of paper maps. These maps were digitised, geometrically rectified and the data then processed through a spatial geographical information system (GIS) database. Infra-red line scans of fire perimeter location at given times obtained from the Country Fire Authority (CFA) and Department of Sustainability and Environment (DSE) in the state of Victoria were used to reconstruct some of the major fires between the years 2000 and 2007. Accounts of fire progression typically came from direct observations made by experienced fire suppression personnel, as recorded in logbooks and radio logs. The database also included more detailed fire reconstruction information from recent wildfire events such as the 2009 Black Saturday fires (Teague et al., 2010; Cruz et al., 2012).

The forward rate of fire spread measurement (R, km h^{-1}) for a given time interval is the maximum R for the interval, determined as $R = d/t$, where d represents the maximum distance (km) from the end point of one fire isochrone to the end point of the preceding isochrone and t is the time period (h) between isochrones. For some bushfires, no fire progression maps could be retrieved, but R measurements were documented in the form of reports.

2.1.2. Weather data and fuel moisture content

Weather data was obtained from the Australian Bureau of

Meteorology's automatic weather station (AWS) network records and from reports which present data taken from manual weather stations located closest to the fire incident. Base data included air temperature, relative humidity, rainfall history, and mean 10-m open wind speed (U_{10}, km h^{-1}) and direction. In certain instances, weather observations were made some distance from the fire, and thus the actual fire conditions may have been significantly different to that indicated by the weather observations. For each wildfire spread period considered between two isochrones, the corresponding weather data was taken as the average meteorological conditions over the time interval.

Field measurements of fine dead fuel moisture content (*MC*, % oven-dry weight) were not available for the wildfires analysed. *MC* was in turn estimated from air temperature and relative humidity using models for eucalypt forests (Matthews et al., 2010).

2.1.3. Vegetation and fuel data

The area enclosed by each wildfire isochrone was classified as either dry eucalypt forest or wet eucalypt forest. This information was derived from the original fire reports and state vegetation maps. Dry eucalypt forests (and woodlands) typically consist of multi-aged stands of a mix of eucalypts and have an understorey dominated by hard-leaved shrubs, grasses, sedges or bracken fern. Wet eucalypt forests typically consist of a tall eucalypt overstorey of multi-aged and mixed species, and a dense understorey of ferns, soft broad-leaved shrubs and small trees.

For wildfires in Victoria, spatially averaged fuel characteristics were determined from a database of ecological vegetation classes and associated age-related fuel accumulation curves (e.g. Walker, 1981), allowing fuel characteristics such as load and fuel hazard by understorey component (Hines et al., 2010) to be estimated at a given site for any given year. For other states, these fuel characteristics were determined from reports and estimated through visual examination of photographs using the Hines et al. (2010) fuel hazard rating and Gould et al. (2007) fuel hazard score assessment guides.

2.2. BONFIRE database

Fernandes et al. (2020) surveyed peer-reviewed articles, grey literature and unpublished data on file to develop a global fire behaviour database encompassing information from experimental fires, prescribed fires and wildfires. In the current analysis, we focused solely on the wildfire component of the database. The following information was retrieved for each fire: georeferenced location, broad vegetation type (i.e. conifer forest, eucalypt forest or shrubland), dominant species, slope steepness, observed rate of fire spread, fire run duration, air temperature, relative humidity and U_{10}. When available, fuel complex attributes (e.g. fuel loads per size class and live or dead condition, curing or % fine dead fuel, fuel depth or height, fuel layer cover), were also extracted. Given the diversity of sources, the dataset is somewhat variable in its completeness.

As part of the post-processing of data, *MC* values were estimated from air temperature and relative humidity using vegetation/fuel type specific models. This included Matthews et al. (2010) for eucalypt forest, the parameterization of this model for semi-arid shrublands given in Cruz et al. (2010), Anderson et al. (2015) for temperate shrublands and conifer forest with a prominent shrub layer. For other conifer forests we used the Rothermel (1983) fuel moisture tables to ensure consistency with the data used by Cruz and Alexander (2019) for this vegetation/fuel type. The BONFIRE data used in the current study is given in Table A2 of the Appendix.

2.3. Imposed data constraints and reliability

Several criteria were imposed on the datasets selected for the analysis to ensure compatibility with the intended use of the 10% rule of thumb. Data used in the analyses originated from wildfire runs lasting at least 1.0 h, but less than 6.0 h. Wildfires that were affected by frontal passage driven wind changes (e.g. Cruz et al., 2012) that altered the dynamics of the fire propagation process (Blanchi et al., 2014) were not considered as the rule of thumb is not applicable to these situations (Cruz and Alexander, 2019). We also restricted the analyses to wildfires meeting the high wind (i.e. $U_{10} > 30$ km h^{-1}) and low fuel moisture (*MC* <7%) conditions where the rule of thumb has shown to be most applicable (Cruz and Alexander, 2019). None of the wildfires used in the original formulation of the 10% rule of thumb (Alexander and Cruz, 2006; Cheney et al., 2012; Anderson et al., 2015) were considered in the present analyses.

Kilinc et al. (2012) and Fernandes et al. (2020) assigned wildfire data reliability scores for weather, fuel and fire behaviour characteristics as per Cheney et al. (2012) and Cruz et al. (2012). This is provided in Tables A1 and A2, respectively. Interpretation of the reliability scores is given in Table A3.

2.4. Predicted fire spread rate data

We applied the 10% rule of thumb to the U_{10} values in both datasets to produce estimates of *R* for each wildfire. We also used the predictions from the McArthur (1967) and Cheney et al. (2012) fire spread models in the Southern Australia dataset to understand how the rule of thumb predictions compare with those of current operational fire spread models under heightened fire spread potential conditions. Predictions for the McArthur (1967) model relied on an overall understorey fuel load comprised of surface, near surface, elevated and bark fuels. Similar analysis was not pursued for the BONFIRE dataset due to the absence of the necessary fuel information needed to apply the appropriate fire spread models.

2.5. Statistics

Model error predictions were quantified using the following statistics: mean absolute error (MAE), mean bias error (MBE), mean absolute percent error (MAPE), root mean square error (RMSE) and the ratio between the MBE and MAE, which we call the mean bias percent error (MBPE) (Willmott, 1982; Cruz et al., 2018).

The MAE, expressed in the same units as the original data, is a quantity used to measure how close predictions are to the observed value. As the name suggests, the MAE is an average of the absolute error. The MBE describes the dispersion or spread of the residual distribution about the estimate of the mean. A positive value indicates an over-prediction trend while a negative value is an indication of an under-prediction trend. The MAPE is a very popular measure of the accuracy of a predictive model or system. It represents the summed differences between the individual predicted versus observed values divided by the observed value and expressed as a percentage. If a perfect fit is obtained, then the MAPE is zero. The MBPE provides a measure of the bias in relation to the MAE expressed as a percentage.

The RMSE represents the standard deviation of the residuals (prediction errors); residuals are a measure of how far from the line of perfect agreement the data points lie. The RMSE is a measure of how spread out these residuals are.

The analysis of the rule of thumb error was conducted separately for the Southern Australia and BONFIRE datasets, despite certain

commonalities, namely data from wildfires in Australian eucalypt forests. The data were not pooled together due to the different data collection methods, standards and overall data characteristics. We analysed differences in fire environment variables for subsets of datasets through unpaired two sample tests. The Shapiro-Wilk test of normality was used to determine if variables were normally distributed. For normally distributed variables Student t-tests were used. For non-normal distributions the non-parametric Wilcoxon rank sum test was used. All statistical analysis was conducted using the software R (R Core Team, 2019).

3. Results

3.1. Southern Australia dataset

The original Southern Australia database consisted of 183 fire observations in eucalypt forests. The dataset selected for analysis was reduced to 61 wildfire observations after removing fire runs with a duration of less than 1.0 h and cases of post-frontal passage type of fire propagation. Within those, a total of 30 fire runs had an estimated *MC* <7% and a measured $U_{10} > 30$ km h^{-1}. For this subset, the average rate of fire spread was 3.6 km h^{-1}, spanning a range of 0.8–8.0 km h^{-1}. Table 1 provides the basic statistics for the subset of data used in this study. The 10% rule of thumb predicted the dataset with a MAE of 1.75 km h^{-1}, and a MBE of 0.89 km h^{-1} (Table 2).

Fig. 2 shows the rule of thumb predictions clustered around two different areas. There is a group of fires ($n = 10$) propagating with a forward rate of spread less than 2.0 km h^{-1} that were characterized by a strong over-prediction bias. The remaining two-thirds of the data, with higher rates of spread, had predictions that mostly fell within the ±35% band. The wildfires in the over-predicted group were slower spreading. The Shapiro-Wilk test of normality showed *MC*, U_{10}, fuel loads and fire front width in each subset of data (i.e. slower spreading wildfires with $R < 2.0$ km h^{-1} *vs* faster spreading wildfires with $R > 2$ km h^{-1}) to not be normally distributed. The slower spreading wildfires were characterized by higher *MC* levels (mostly 5–6%, averaging 5.3%) than the dataset average of 4.4%. The Wilcoxon rank sum test indicated *MC* to be significantly higher in the slower spreading group than in the faster spreading group ($p = 0.008$). The same test found no statistically significant differences for wind speeds and fuel loads in the two groups ($\alpha > 0.05$). Fire front width was larger in the faster spreading wildfires (4.3 km) than in the slower spreading group of fires (1.6 km), with the Wilcoxon rank sum test finding the differences significant ($p = 0.004$). Considering only the wildfires spreading with a $R > 2.0$ km h^{-1}, the use of the rule of thumb resulted in an MAE of 1.04 km h^{-1}, MAPE of 22.4% and a MBE of 0.24 km h^{-1}.

Predictions of rate of fire spread with the McArthur (1967) and Cheney et al. (2012) models yielded higher MAEs (2.12 and 2.19 km h^{-1}, respectively) than the rule of thumb, albeit showing distinct trends (Fig. 2). The McArthur (1967) model largely under-predicted the spread of the wildfires, with an MBE (−2.03 km h^{-1}) of similar absolute magnitude to the MAE (Table 2), whereas the Cheney et al. (2012) model yielded a negligible bias (MBE of −0.02 km h^{-1}). Both of these

Table 1
Summary of basic statistics for observed rate of fire spread (R), 10-m open wind speed (U_{10}) and estimated fine dead fuel moisture content (MC) of the Southern Australia wildfire dataset (Kilinc et al., 2012) in Australian eucalypt forests meeting the study requirements (n = 30). Data distribution by state: Victoria (25); Western Australia (4); and South Australia (1).

Variable	Mean (st.dev.)	Range
R (km h^{-1})	3.6 (2.01)	0.8–8.0
U_{10} (km h^{-1})	45.2 (12.3)	30–100
MC (%)	4.4 (1.3)	2.5–6.2

Table 2
Summary of the evaluation statistics for predicted rate of fire spread models for the Southern Australia wildfire dataset (Kilinc et al., 2012) in Australian eucalypt forests meeting the study requirements. MAE – mean absolute error; MBE – mean bias error; MAPE – mean absolute percent error; RMSE – root mean square error; and MBPE – mean bias percent error. Residuals are calculated as predicted-observed, with a negative MBE indicating an under-prediction.

Rate of fire spread model	MAE (km h^{-1})	MBE (km h^{-1})	MAPE (%)	RMSE	MBPE (%)
Cruz and Alexander (2019)	1.75	0.89	101.0	2.11	51
Cheney et al. (2012)	2.19	−0.02	76.9	2.72	-1
McArthur (1967)	2.21	−2.03	60.0	2.95	−92

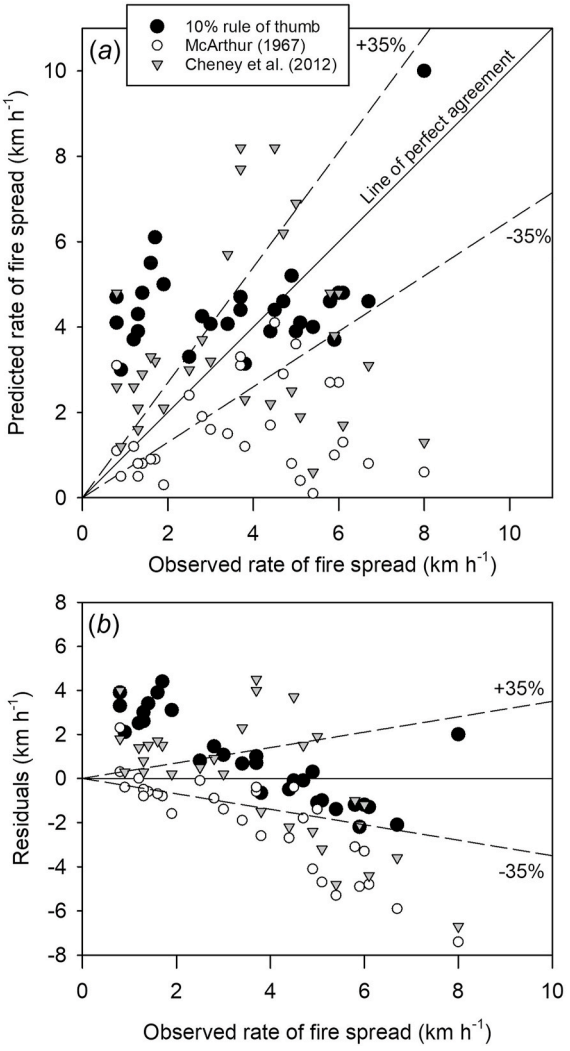

Fig. 2. Plots of (a) observed rates of wildfire spread in Australian eucalypt forests for the Kilinc et al. (2012) dataset meeting the study requirements versus predicted values according to the Cruz and Alexander (2019) 10% rule of thumb and the models of McArthur (1967) and Cheney et al. (2012) (the dashed lines around the line of perfect agreement indicates the ±35% error interval as per Cruz and Alexander, 2013) and (b) residual distribution as a function of observed rate of wildfire spread.

Table 3
Summary of basic statistics (mean, (standard deviation), [range]) for observed rate of fire spread (R), 10-m open wind speed (U_{10}), estimated fine dead fuel moisture content (MC), and country of origin for the BONFIRE (Fernandes et al., 2020) wildfire dataset meeting the study requirements.

Variable	Conifer forests[a]	Eucalypt forests[b]	Shrublands[c]	All[d]
R (km h^{-1})	3.9 (2.84) [0.6–12.5]	4.4 (3.09) [0.8–11.2]	3.7 (1.93) [1.1–7.5]	4.0 (2.70) [0.55–12.50]
U_{10} (km h^{-1})	45.6 (15.1) [30–80]	48.4 (12.0) [30–70]	40.2 (9.7) [33–73]	45.6 (12.9) [30–80]
MC (%)	6.1 (0.65) [4.0–7.0]	3.4 (0.49) [2.6–4.5]	4.4 (1.57) [2.2–6.6]	4.6 (1.52) [2.0–7.0]

[a] $n = 21$. Data distribution by country: Argentina (3); Australia (6); Canada (2); Greece (1); New Zealand (3); Portugal (2); Spain (2); and USA (2).
[b] $n = 22$. Data distribution by country: Australia (21) and Portugal (1).
[c] $n = 15$. Data distribution by country: Argentina (1); Australia (5); Portugal (5); Spain (2); and USA (2).
[d] $n = 58$. Data distribution by country: Argentina (4); Australia (32); Canada (2); Greece (1); New Zealand (3); Portugal (8); Spain (4); and USA (4).

models produced more accurate predictions for the slower spreading fires ($R < 2.0$ km h^{-1}), but higher errors for the faster spreading ones (Fig. 2b). The Cheney et al. (2012) model over-predicted the rate of advance of all wildfires in the slower spreading group (Fig. 2b).

3.2. BONFIRE dataset

The BONFIRE database compiled by Fernandes et al. (2020) contained a total of 167 wildfire runs in non-grass fuels, with a run duration >1.0 h, not classified as post-frontal passage fire propagation, nor included in the datasets used to derive the rule of thumb (i.e. Alexander and Cruz, 2006; Cheney et al., 2012; Anderson et al., 2015) and not present in the Southern Australia dataset. Within that dataset, there were a total of 58 fire observations in conifer forests, eucalypt forests and shrublands that met the criteria of the MC <7% and $U_{10} > 30$ km h^{-1}. The basic statistics for this dataset are given in Table 3, including the distribution by geographic location. The R for these datasets averaged 4.0 km h^{-1}, with the distribution of this variable, MC and U_{10} not significantly different from the Southern Australia dataset. Tukey multiple comparison tests indicated no significant differences between the R in the three broad vegetation/fuel types present in the dataset. Comparable results were obtained for U_{10}, but significant differences ($p < 0.05$) were observed for the MC.

The application of the 10% rule of thumb resulted in a MAE of 1.70 km h^{-1} (Table 4) when considering the aggregate of the three vegetation/fuel types, a value comparable to the one obtained for the Southern Australia dataset. The 10% rule of thumb predicted R values for the dataset with a MBE of 0.49 km h^{-1} or 29% of the MAE (Table 4). Overall the most accurate predictions were obtained for the shrubland subset (MAE 1.54 km h^{-1}, MAPE 59.6%), followed by the conifer forest subset (MAE 1.55 km h^{-1}, MAPE 80.3%) and then the eucalypt forest subset (MAE 1.95 km h^{-1}, MAPE 89.3%) (Table 4).

As with the Southern Australia dataset, the analysis shows a notable over-prediction bias for wildfires propagating with rates of spread <2.0

Table 4
Summary of evaluation statistics by fuel type for predicted rate of fire spread by the 10% rule of thumb for the BONFIRE dataset (Fernandes et al., 2020). MAE – mean absolute error; MBE – mean bias error; MAPE – mean absolute percent error; RMSE – root mean square error; and MBPE – mean bias percent error. Residuals are calculated as predicted-observed.

Vegetation/fuel type	MAE (km h^{-1})	MBE (km h^{-1})	MAPE (%)	RMSE	MBPE (%)
Conifer forests	1.55	0.63	80.3	1.88	41
Eucalypt forests	1.95	0.48	89.3	2.24	26
Shrublands	1.54	0.28	59.6	1.85	18
All	1.70	0.49	78.1	2.01	29

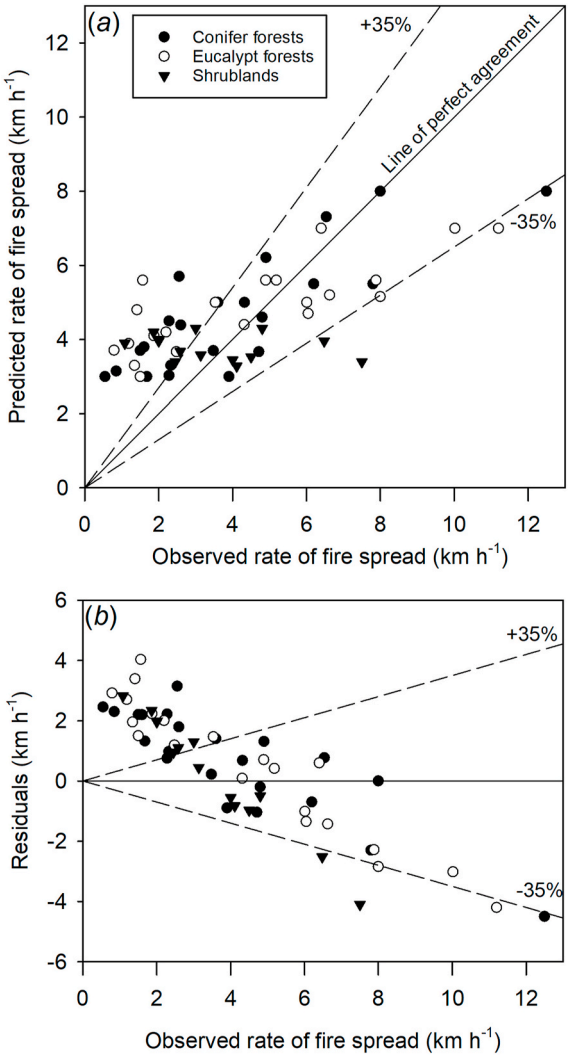

Fig. 3. Plots of (a) observed rates of wildfire spread by vegetation/fuel type for the BONFIRE dataset (Fernandes et al., 2020) meeting the study requirements versus predicted values according to the Cruz and Alexander (2019) 10% rule of thumb (the dashed line around the line of perfect agreement indicates the ±35% error interval as per Cruz and Alexander, 2013) and (b) residual distribution as a function of observed rate of wildfire spread.

km h^{-1} (Fig. 3). A large proportion of the fires spreading with an R between 2.0 and 8.0 km h^{-1} were predicted within the ±35% error prediction band. The rule of thumb tended to under-predict fires spreading with an $R > 7.5$ km h^{-1}, although errors for these fires were around the −35% threshold (Fig. 3).

4. Discussion

4.1. Fire spread prediction error

The spread of a wildfire flame front comprises very dynamic phenomenon, influenced by a number of variables and processes. Its prediction in an operational setting, over a period of hours to days, is fraught with uncertainty associated with the limitations of our understanding of the controlling processes, difficulty in accurately estimating a model's input variables, compounding effects of errors and the obvious difficulty in describing the chaotic nature of fluids in a turbulent and constantly changing environment (Albini, 1976).

Catchpole et al. (1993) report that measured rates of fire spread in replicated (i.e. same environmental conditions) laboratory experimental fires conducted under constant wind speed conditions agreed to within ±20% (Fig. 4A). This result can be seen as a benchmark with respect to fire spread variability. Spreading fires will exhibit notable variability even when burning in a controlled environment under homogeneous and identical conditions. Outdoor fires, but especially wildfires, will obviously be characterized by a higher variability given the transient and dynamic nature of boundary layer meteorology, plus the spatial variability in fuel characteristics (e.g. structure, moisture) and terrain (e.g. slope steepness, aspect or slope exposure).

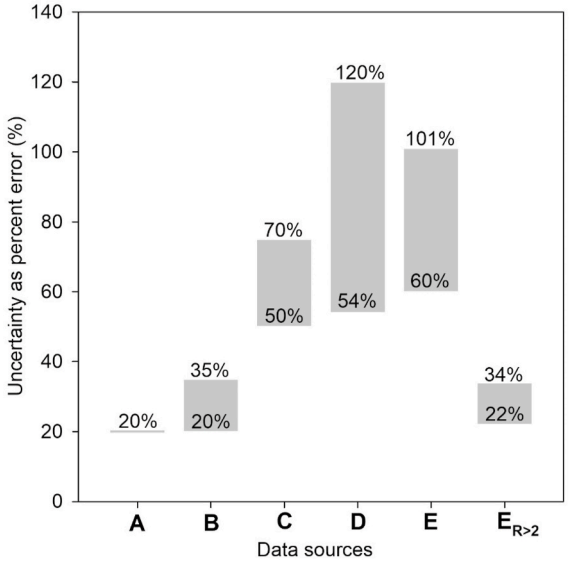

Fig. 4. Error associated with fire spread variability and prediction as quantified in different studies: A – replicability of fires conducted under fixed and controlled conditions in a wind tunnel (Catchpole et al., 1993); B – range in mean absolute percent error (MAPE) obtained when empirically derived models are used to predict the original datasets in grasslands (Cheney et al., 1998), shrublands (Fernandes, 2001), conifer forests (Cruz et al., 2005; Fernandes et al., 2009) and eucalypt forests (Cheney et al., 2012); C – MAPE for studies within the interquartile error range ($n = 23$) where fire spread models were evaluated against independent experimental fire data analysed by Cruz and Alexander (2013); D - MAPE found for studies evaluating fire spread models against independent wildfire data (Alexander and Cruz, 2006; Cheney et al., 2012; Kilinc et al., 2012; Anderson et al., 2015); E – range in MAPE obtained when applying the Cruz and Alexander (2019) 10% rule of thumb to the Southern Australia (Kilinc et al., 2012) and BONFIRE (Fernandes et al., 2020) datasets meeting the present study requirements; and $E_{R>2}$ – range in MAPE obtained when restricting the data in E to wildfires with observed rates of spread >2.0 km h^{-1}.

The most accurate results obtained with empirical models in a field setting are for model predictions against the datasets used in their development, with MAPEs varying between 20 and 35% (Cheney et al., 1998, 2012; Fernandes, 2001) (Fig. 4B). Prediction errors naturally increase when the models are applied to independent experimental fire (Fig. 4C) or wildfire (Fig. 4D) datasets. In these cases, the MAPE has been characterized by an interquartile range varying from 50 to 70% for experimental fire datasets (Cruz and Alexander, 2013) and from 54 to 120% for wildfire data (Alexander and Cruz, 2006; Cheney et al., 2012; Kilinc et al., 2012; Anderson et al., 2015). The main reason for the error increase in the latter dataset is due to the large uncertainty in spread rate measurements, model inputs and the natural unaccounted variability in the fire environment associated with large wildfire runs (Cruz and Alexander, 2013, 2019; Coen et al., 2018).

Considering the spread of fires under critical fire weather conditions, our analysis was based on a broader dataset ($n = 88$) than the original work by Cruz and Alexander (2019) that included only 24 wildfire runs (out of 118 observations) within the constraints of $MC < 7\%$ and $U_{10} > 30$ km h^{-1}. The results obtained by the simple 10% rate of spread rule of thumb as analysed in the present study, with the MAPE varying between 60 and 101% (Tables 2 and 4), is, first and foremost, indicative of the strong control wind speed alone exerts on landscape-scale fire propagation under dry fuel conditions. This despite the uncertainty in the use of measured wind speed data as being representative of the conditions driving a wildfire some distance away from the measurement location.

As observed in the analysis of Cruz and Alexander (2019), the percent error associated with the rule of thumb predictions decreases substantially with the increase in R. The MAPE varied between 22 and 34% when considering wildfires that were propagating with an $R > 2.0$ km h^{-1}, the wildfires that are most dangerous from the point of view of community and fire-fighter safety. This error is on par with the error obtained by empirical-based fire spread models when assessed against their original datasets with *in situ* accurate measurements of the fire environment (e.g. Cheney et al., 1998; Fernandes, 2001).

The results presented in Figs. 2 and 3 raise the question of why does the 10% rule of thumb work so well under certain conditions and not so well in others? The analysis showed a substantial over-prediction for wildfires observed to spread with an $R < 2.0$ km h^{-1}, independent of the dataset. A similar over-prediction bias for wildfires in this range of observed rate of spread was noted in the original analysis by Cruz and Alexander (2019). In the Southern Australia related dataset, this bias was related to fireline width and time of day (mostly early-to mid--afternoon fire runs). This hints at the notion that early afternoon conditions reflect the fact that longer timelag fuels (Nelson, 2001) are not yet fully available for combustion and the possible impact of effective suppression (Plucinski, 2019a, 2019b) in some areas around a wildfire's perimeter, could explain the smaller fireline width and the lower observed rates of fire spread relative to the 10% rule of thumb expectation. Unfortunately, the BONFIRE dataset did not have the detail necessary to further explore this issue.

These results highlight some of the limitations of the 10% rule of thumb, namely that its best accuracy might be restricted to lower *MC*

levels than proposed by Cruz and Alexander (2019). In their analysis, it was suggested that the rule of thumb worked best below an *MC* of 7%, while the current analysis with a broader dataset indicates that the most accurate results are obtained with a *MC* level up to 5%.

The analysis of the BONFIRE related dataset identified an under-prediction trend for wildfires spreading with an $R > 7.5$ km h^{-1}. There were eight fires in this group, with seven under-predictions, six of them with under-predictions varying between −29% and −38%, and one of them with a −55%. A closer review of these wildfires reveals a prevalence of documented long-range spotting distances in most of them, namely the 1983 Deans Marsh fire (10 km spotting - Rawson et al., 1983) and the East Trentham fire (10–12 km - Rawson et al., 1983; Storey et al., 2020b) in Victoria, Australia, the 1936 Galatea Creek Fire in Alberta, Canada, (5.6 km - Fryer and Johnson, 1988), and the 1983 Mount Muirhead fire in South Australia (15–20 km - Keeves and Douglas, 1983).

Long-range spotting is a highly stochastic process linked to a number of variables such as the size of the active fire area, fuel type(s), terrain roughness, wind speed levels and wind exposure (Page et al., 2018; Storey et al., 2020a). The processes are heuristically understood, with long-range spotting associated with wind-driven wildfires typically linked to fires accelerating in wind exposed upslope runs. This results in localised increases in energy release, an increase in the number of firebrands generated, and pulses in upward momentum in a wildfire's plume (Kerr et al., 1971; Luke and McArthur, 1978; McCarthy et al., 2018). These periodic pulses are able to transport firebrands higher into the wildfire's plume where upper levels winds can then maximise their downwind transport (Albini et al., 2012). However, not all upslope fire runs will lead to the long-range spotting as observed in the wildfires mentioned above.

The results obtained seem to indicate that if the fire environment is conducive to the occurrence of long-range spotting distances, then the 10% rule of thumb will likely under-predict the overall fire spread distance. In our evaluation, the level of under-prediction was between 30 and 40%, which is fairly acceptable given the uncertainty in the input variables and the stochasticity of the process, although higher under-prediction errors cannot be ruled out. The fact that the 10% rule of thumb predicted well wildfires driven by winds of 60–70 km h^{-1} (with gusts up to around 100 km h^{-1}) and characterized by long-range spotting with errors up to 40%, is in itself a very interesting result.

4.2. Fire spread prediction error - operational implications

As simulations of fire spread models are used to support decision making during ongoing wildfires, it is important that the users of such information understand the uncertainty in fire spread predictions, either due to errors associated with inaccurate inputs or model limitations (Albini, 1976). Despite the complexity of wildfire phenomena, the unknowns in our scientific understanding of fire behaviour and the chaos associated with a wildfire approaching the WUI, to the individuals making decisions regarding the safety of communities or fire-fighters in the field, the questions are very simple: where is the wildfire at the moment and what is its rate of spread and intensity (Luke and McArthur, 1978)? Will the wildfire reach a particular community or pre-defined trigger point and at what time will it do so (Cova et al., 2005; Ramirez et al., 2019)? The decision maker will need to understand the uncertainty and potential bias associated with the fire spread prediction to make better decisions and tailor the actions to be taken.

Fig. 5 summarises the impact of a rate of spread prediction error on a hypothetical example of a wildfire starting 6.0 km upwind of a community. The example assumes that 0.5 h after ignition, the wildfire is spreading at 3.0 km h^{-1}. For the sake of simplicity, the wildfire is assumed to have been detected the moment following ignition and that in the early stages of fire propagation (i.e. during its build-up phase), the fire was spreading at the pseudo steady-state rate of spread (Luke and McArthur, 1978). The example considers the wildfire to impact the community 2.0 h after ignition and that a fire behaviour analyst produced a forecast of fire spread 0.5 h after the ignition was detected and the local authorities act upon this information to immediately release a warning to the general public. If a correct *R* prediction of 3.0 km h^{-1} is made (i.e. 0% error) and an evacuation warning is issued, then the population has 1.5 h to act before the wildfire impacts the community. Over-predictions will result in a reduction in the perceived time to impact (i.e. the community will think that they have less time to act than in reality). With an increase in an over-prediction, the predicted time to impact decreases to a level that might lead to a negative outcome (area A in Fig. 5), e.g. emergency services decide that the time for a community to safely evacuate is too short and thus do not issue an evacuation warning. This is clear for the 100% over-prediction error (a *R* prediction of 6.0 km h^{-1}), where a predicted time to impact of 0.5 h might lead to a change from evacuation to a "shelter-in-place" warning. Such advice against evacuation when time does allow for its safe implementation can potentially put members of the general public at undue risk.

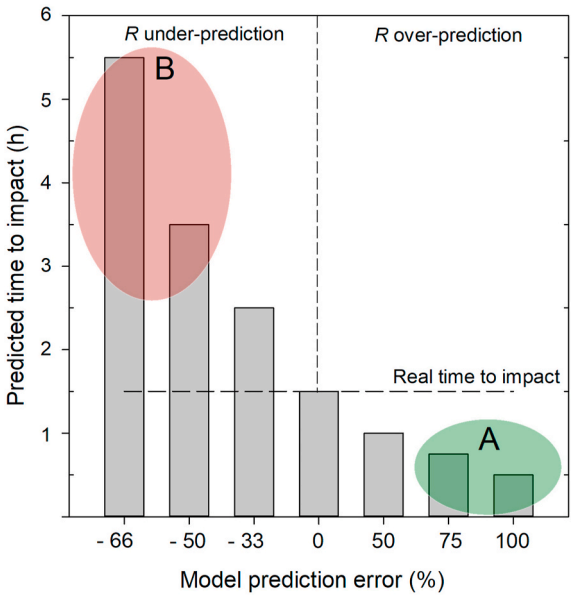

Fig. 5. Effect of fire spread model prediction percent error in the predicted time to impact for a hypothetical wildfire impacting a community 1.5 h after a real-time fire behaviour prediction is completed. A and B are regions where the magnitude of the error can result in negative impact on the decision making.

Under-prediction biases of wildfire rate of spread can also have a detrimental, but distinct, impact on the decision-making process. Under-predictions will result in an erroneous over-estimate of the time to fire impact, potentially removing the necessary sense of urgency (area B in Fig. 5). For example, the largest under-prediction in Fig. 5 suggesting 6.0 h to impact might delay any warnings to the general public during a

Box 1
Synopsis of recent notable wildfire events around the world characterized by rapid spread and a significant number of human fatalities. See Table 5 for further details and associated references.

2009 Kilmore East fire, Victoria, Australia.

The Kilmore East fire started at approximately 11:45 as a result of arcing from a broken power line. The fire, burned approximately 100 000 ha in less than 12 h, causing 121 fatalities and injuring 232 people (Teague et al., 2010; Cruz et al., 2012). The fire had two distinct spread periods, with the first being a wind driven run pushed by hot dry winds averaging 28–69 km h^{-1} (Fig. 1b), followed by the second period characterized by the passage of a cold front at 18:00 that turned a 55 km long flank fire into a headfire. Focusing on the pre-frontal passage period, which caused 58 of the fatalities, the fire travelled 55 km through predominantly forest fuels in approximately 6 h, for an average rate of spread of 9.2 km h^{-1}. This extraordinary fast rate of spread was associated with profuse spotting characteristic of high-intensity fires spreading in eucalypt forests.

2017 Tubbs fire, California, USA.

The Tubbs fire was caused by an electrical system failure at 21:43 on October 8, 2017 (Koslowsky, 2019). Pushed by strong, downslope diablo winds (Bowers, 2018; Coen et al., 2018; Smith et al., 2018), the fire impacted several communities in the first 4–5 h of fire propagation following ignition, causing 22 fatalities and the destruction of 5636 structures (Nauslar et al., 2018). Over this period of time, average wind speeds (measured at 6.1 m) in weather stations in the vicinity of the fire ranged from 32 km h^{-1} at Santa Rosa in the valley in the vicinity of the fire's path to 70 km h^{-1} on a ridgeline about 20 km northwest of the fire. Rates of spread as the fire propagated towards Santa Rosa between 23:00 on October 8 and 02:00 on October 9 ranged between 2.98 and 5.24 km h^{-1}, for an overall average of 3.9 km h^{-1} for the approximate 4.0 h run of 16.7 km.

2017 Arganil-Seia fires, central Portugal.

The Arganil-Seia fire complex caused 17 fatalities, making it the deadliest of those fires starting on October 15 in Portugal under the influence of Ophelia's tropical storm winds and the associated advection of warm and dry air from northern Africa (Guerreiro et al., 2018). The fire complex comprised four separate ignitions that merged together, burning 48 462 ha, half of which was occupied by pine forest. However, the fire run referred to in Table 5, that started at 12:28 was the result of a rekindling of part of the initial fire growth from the previous week. This run initially advanced with an average spread rate of 1.8 km h^{-1}, followed by a sustained propagation of 4.5 km h^{-1} between 15:00 and 17:00 as wind speeds increased. Rate of spread was substantially reduced as the fire encroached into the wildland-urban interface of the Oliveira do Hospital township, and increased subsequently, with an average spread rate of 5.4 km h^{-1} between 20:00 and 24:00. This later period was marked by prolific spotting in a more fragmented forest landscape.

2018 Mati fire, Attica region, Greece.

The Mati fire started at 16:41 on July 23, 2018. Strong winds, ranging between 32 and 56 km h^{-1} in an exposed mountainside AWS site west of the ignition area, and 24–30 km h^{-1} at a coastal AWS site (Table 5) lead to a fast downslope run over complex topography toward several seaside communities, with the wildfire reaching the sea at approximately 18:30. This run resulted in 102 fatalities, with the wildfire also impacting 1650 homes within a final burned area of 1431 ha (Goldammer et al., 2019; Xanthopoulos and Athanasiou, 2019; Lagouvardos et al., 2019). Reconstruction of the wildfire propagation indicated an overall rate of fire spread of 2.6 km h^{-1} from the ignition point to the sea shore (a distance of 5.2 km), although the flame front was documented to be spreading at 4.0 km h^{-1} over the latter half of its run, with peak spread rates of up to 5.0 km h^{-1} over shorter distances.

2018 Camp fire, California, USA.

The Camp fire was ignited by a faulty electric transmission line at 06:33 on November 8, 2018 near Pulga, California (Gee and Anguiano, 2020). Driven by strong, foehn winds, the wildfire spread rapidly in open chaparral shrublands and conifer forest fuel types during its first morning of activity, severely impacting several communities, including the town of Paradise, leading to 86 fatalities and the destruction of more than 18 000 buildings. Detailed weather analysis by Brewer and Clements (2019) indicate that the average measured surface wind speeds (6.1 m height) in the vicinity of the fire perimeter varied between 18 and 54 km h^{-1} with gusts up to 94 km h^{-1}. These authors also suggest a strong gradient of wind speed with height with substantially higher wind speeds aloft contributing to long-distance ember transport (spot fires were observed occurring 1.5 km ahead of the main flame front. The Landsat 8 image of the wildfire taken at 10:45 (Fig. 1c) shows the leading edge of the main fire's footprint covering a distance of 16.9 km from the point of ignition. This yields a rate of fire spread of 4.0 km h^{-1}. If one considers the further extent of a large spot fire located 20.1 km from the ignition point observed in the satellite image, the wildfire would be considered to have advanced at a rate of 4.8 km h^{-1} over this initial 4:12 h period of spread. The headfire spread a further 7.2 km by around 18:00, resulting in an average rate of spread of 1 km h^{-1} for the period from 10:45 to 18:00.

critical time period. Considering 1.0 h as a time scale relevant for community evacuation (Li et al., 2019), errors up to 33% are not likely to have a detrimental impact on public safety. It is errors above this threshold, and in particular under-prediction errors, that can result in a lack of timely and appropriate warnings leading to the most detrimental consequences (Cheney, 1981; Teague et al., 2010).

4.3. Performance of the 10% rule of thumb against five notable recent wildfire disasters

The recent past is populated with some of the deadliest single wildfire events on record (Box 1). Common features of these wildfires were, for example: a new ignition starting the deadly fire run (with the exception of the 2017 Arganil-Seia fire), strong winds leading to fast spread rates, impact into communities within a few hours of their

Table 5
Summary regarding the details on the occurrence, fatalities, behaviour and environmental conditions associated with five notable wildfire disasters globally in recent times. T_a – ambient temperature; *RH* – relative humidity; *MC* – fine dead fuel moisture content; U_{10} – 10-m open wind speed; and *R* – rate of fire spread including that predicted by the 10% rule of thumb. For further details refer to Box 1.

Fire name and location	Date	Number of fatalities	Duration of run (h)	Time to bulk of fatalities (h)	T_a (°C)	*RH* (%)	*MC* (%)	U_{10} (km h^{-1})	Observed *R*(km h^{-1})	Predicted *R* (km h^{-1})
Kilmore East, Australia	February 07, 2009	121[a]	6	4–5	45	8	5	28–69	4.1–9.2	2.8–6.9
Tubbs, USA	August 10, 2017	22	4	3–4	33	7	5	32–70	3.0–5.2	3.2–7.0
Arganil-Seia, Portugal	October 15, 2017	17	2	4–5	33	17	6	19–49	4.4-4.6	1.9–4.9
Mati, Greece	July 23, 2018	102	2	2	38	17	5	32–52	2.6–5.2	3.2–5.2
Camp, USA	November 08, 2018	86	4	3–4	11	19	8	21–62	4.0–4.8	2.1–6.2

Kilmore East fire observations: U_{10} range based on the two closest Australian Bureau of Meteorology automated weather stations at Kilmore Gap (near the ignition point, characterized by higher wind speeds) and Coldstream (a few km from the end of the considered run, characterized by lower wind speeds). Other environmental data and rate of fire spread are from Cruz et al. (2012).
Tubbs fire observations: Wind speeds measured at 6.1-m height at Santa Rosa (lower wind speeds) and Hawkeye (higher wind speeds) automated weather stations (AWS) (https://mesowest.utah.edu) were converted to U_{10} values as per Andrews (2012). The Santa Rosa AWS is located in the valley near the vicinity of the fire's path. The Hawkeye AWS is located along a ridgeline about 20 km northwest of the fire (Coen et al., 2018). T_a, *RH* and *MC* are representative of the Santa Rosa AWS. Rates of fire spread derived are from Watkins et al. (2017) and Monedero et al. (2019) per data supplied by the California Department of Forestry and Fire Protection.
Arganil-Seia fire observations: Wind speeds measured in the Fajão wind farm at a 80 m height, located on a ridgeline 12 km south of the fire run. 10-min observations from 37 anemometers were averaged for the fire run period and converted to U_{10} values based on a logarithmic wind profile (Tennekes, 1973) assuming a 0.4-m surface roughness. High atmospheric instability implied an underestimation by the conversion but it is expected that the corresponding U_{10} at the fire location would be somewhat lower, given the 300-m elevational difference. Rates of fire spread are from Guerreiro et al. (2018).
Mati fire observations: Wind speed data is the average for the period of the fire run for the Rafina AWS (coastal site, lower wind speeds) and Pentelli (mountain site, higher wind speeds) automated AWS (Lagouvardos et al., 2017). The Pentelli AWS is located at a mountain top, where air flow is compressed, and winds accelerate. The Rafina AWS is located 2 km south of where the fire reached the sea. The anemometer at this station is located at a 3-m height atop a building (flat roof). A conversion to U_{10} for this exposure is unclear. The values given above have been adjusted by multiplying the observed values by 1.15 as per Andrews (2012). It is expected that the corresponding U_{10} values at the Rafina AWS would be somewhat higher than estimated, as visual observations in the area suggested a Beaufort scale rating of 7 (~61 km h^{-1}). Other environmental data is representative of Rafina AWS observations. Rates of fire spread are from Goldammer et al. (2019) and Xanthopoulos and Athanasiou (2019).
Camp fire observations: Wind speed range as reported by Brewer and Clements (2019) from data collected in the vicinity of the fire perimeter. U_{10} values incorporates correction factor for 6.1-m to 10-m open wind winds as Andrews (2012). Rates of fire spread based on distance from ignition point to fire perimeter location at 10:45 a.m. based on Landsat imagery (Fig. 1c).
[a] Of the total 121 fatalities, 51 occurred during the main wind-driven fire run with the remaining 70 associated with the post-frontal passage fire propagation (Cruz et al., 2012).

ignition and communities not warned of the impending danger until it was too late to evacuate to safe areas (e.g. Xanthopoulos and Athanasiou, 2019). For most of these wildfires, the lack of a formal warning to the communities prior to fire's impact was due in part to the lack of situational awareness and an under-appreciation of the fire spread rate potential by civil protection/emergency response agencies (Teague et al., 2010; Goldammer et al., 2019).

In complementing the analyses presented in the previous sections, Table 5 provides some additional details on the characteristics of the wildfires listed in Box 1. A feature of the measured wind data reported in Table 5 (note the different standards for the measurement height above ground) for these wildfires is the broad range in the average wind speeds for each of the fires (Fig. 6). Winds were measured at different locations near the vicinity of these wildfires or within the final fire perimeter. Weather stations situated on ridgelines or on windward slopes, generally resulted in the upper range in wind speeds whereas stations located at lower elevations, where the impacted communities typically were, yielded a lower range in wind speeds. These results highlight some of the inherent issues of predicting the spread of wildfires advancing across complex topography.

Detailed wind studies such as those carried out by Coen et al. (2018), Brewer and Clements (2019), and Lagouvardos et al. (2019), for example, further highlight the spatial heterogeneity in landscape-scale winds and the complexities associated with the strong wind events linked to some of the catastrophic wildfires described in Box 1 and Table 5. This also calls attention to the fact that the wind speed data given in Tables A1 and A2 should be seen as indicative, not necessarily as a precise value representative of a large wildfire run.

The 10% rule of thumb yielded estimates that approximate the observed rates of spread of the wildfire disasters (Fig. 6; the wind speed bar can be read as the 10% rule of thumb *R* prediction in the rate of fire spread axis label). The application of the rule of thumb under-predicted the spread rate for the 2009 Kilmore East fire (−26% error when considering the maximum wind speed and the overall rate of fire spread), a result linked to the occurrence of long-range spotting during this fire's major run (Cruz et al., 2012), and over-predicted the maximum spread rate for the 2017 Tubbs fire (35% error), which are clearly errors within an acceptable range for wildfire propagation prediction. Errors for the other wildfires contained in Table 5 were smaller with the range in the predicted rate of spread based on the range in observed wind speeds overlapping the range in observed rate of fire spread (Fig. 6).

We need to emphasize that these results should be seen as qualitative and only as an illustration of the usefulness of the 10% rule of thumb as a first approximation in situations where there is no particular fire behaviour prediction know-how or there is no time to apply more comprehensive and accepted fire behaviour prediction methods (e.g. Rothermel, 1983, 1991; Plucinski et al., 2017; Taylor and Alexander, 2018). The quick usage of the rule of thumb in these situations, when time is of the essence, leaves more time for undertaking other

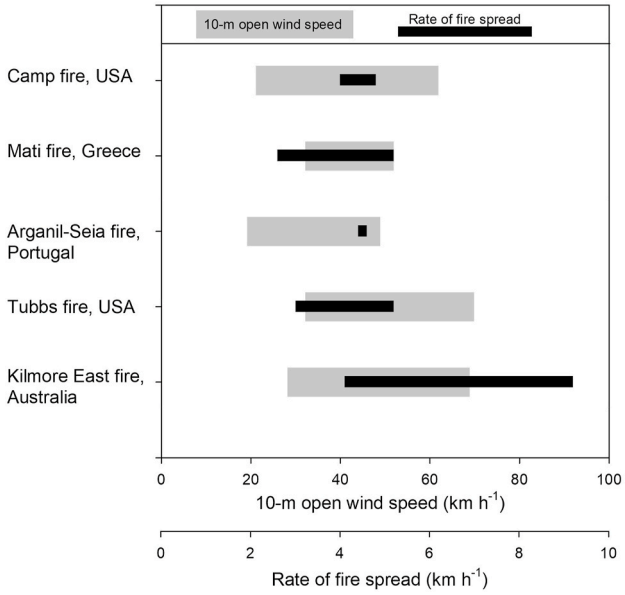

Fig. 6. Temporal and spatial range in reported forward rate of spread and 10-m open wind speed for five recent wildfire disasters involving large numbers of human fatalities. See Box 1 and Table 5 for a brief description of each wildfire and associated environmental details.

time-critical actions, including informing the general population.

The strong control that wind speed exerts on the propagation of wildfire conflagrations, as shown in the analysis of wildfire case studies, highlights the importance of accurate wind forecasting (Coen et al., 2018; Lac et al., 2018; Lagouvardos et al., 2019) and its fine scale spatial modelling (Wagenbrenner et al., 2016; Filippi et al., 2018), especially in complex terrain, to guide effective decision making and issuing of warnings during extreme burning conditions.

4.4. On the wind speed effect on fire propagation

The error analysis resulting from the evaluation of the 10% rule of thumb against independent data has provided additional clues as to the influence of wind speed on wildfire propagation rates. We noted in section 4.2 that a group of the slower spreading fires (i.e. $R < 2.0$ km h^{-1}) were found to be over-predicted by the 10% rule of thumb. Although we did not apply the 10% rule to fires spreading with U_{10} levels <30 km h^{-1} or MC >7% in the present study, the analysis by Cruz and Alexander (2019) found an over-prediction bias for wildfires spreading under these conditions. In contrast, the low percent errors produced for wildfires with observed R levels >2.0 km h^{-1}, hints at the overarching control wind speed exerts on the forward speed of wildfires when fine dead fuels are critically dry and wind speeds are strong. The fit statistics do not leave much room for other influences, be it a forest or shrubland vegetation/fuel type, topographic effects or fire-atmosphere interactions, when wildfires are spreading under these conditions.

Potter (2002) suggested that under strong wind conditions, the convective plume tilt of a wildfire along with the transport of the plume condensation area downwind, will lead to a decoupling between the advancing flame front of the fire at the surface and the plume above. This will limit dynamic feedbacks, such as downdrafts or return flows on the advancing flame front that may arise from the moisture latent heat release in the fire's plume. In these situations, wind speed and fuel dryness control a wildfire's spread rate.

The observed over-prediction for the group of slower spreading wildfires mentioned above, could arise from fire-atmosphere interactions. In situations with lower wind speeds, the fire's convection column is more vertical than in the strong wind case and coupling between the upper levels of the plume and the surface can occur (Byram, 1959; Rothermel, 1991). Air entrainment due to vertical plume development in distinct layers of the atmosphere coupled with moisture condensation will feedback into a free-burning fire as the vertical motions change the near-fire surface winds (Potter, 2002). These feedbacks can result in periodic or occasional strong downdrafts winds that can cause sudden changes in fire behaviour (Potter, 2005; Coen, 2011), occasionally with possible life-threatening consequences (e.g. Rothermel, 1991; Goens and Andrews, 1998). Despite the occasional extreme flows associated with dynamic feedbacks, the strong entrainment into the fire's plume and upward motions will, when considering the time scales used in our study (i.e. greater than 1 h), result in overall lower horizontal winds at the surface. This might possibly explain in part the observed fire spread rates being lower than expected based on the rule of thumb.

5. Conclusions

We conducted an examination of the predictive ability of the Cruz and Alexander (2019) 10% rule of thumb to estimate a wildfire's forward rate of fire spread using two independent datasets. This simple rule of thumb aims to provide first approximations of wildfire propagation for situations where there is little or no time to apply more comprehensive and accepted fire behaviour prediction methods. The rule of thumb was shown to work well, with overall MAPEs between 80 and 100% comparable to other model evaluation studies based on wildfire data. The analysis showed the rule of thumb to work best for fast-spreading wildfires ($R > 2.0$ km h^{-1}). For these cases, the MAPE varied between 22% and 34%, a result on par with error statistics obtained when evaluating empirical-based fire spread models against the data used in their development.

Our analysis showed that the range of conditions where the rule of thumb worked best is possibly more restrictive than originally thought. We found the rule to be most reliable under strong wind ($U_{10} > 30$ km h^{-1}) and dry fine fuel (MC <5% rather than <7%) conditions typically associated with fast-spreading wildfires. It is these types of fires that can surprise communities and emergency response agencies due to their high potential spread rates. The 10% rule of thumb is relevant when landscape-scale dryness is conducive to major wildfire outbreaks – i.e. low moisture content levels for live fuels and dead fuels with long timelag response (e.g. deep duff layers and large-diameter coarse woody debris).

Although the focus of the present work was to evaluate the 10% rule of thumb against wildfire data, the analysis also provided insight into fundamental properties of fires burning under high fire spread potential. Despite the uncertainty and variability in the data, the trends are clear – wind speed has an overwhelmingly dominant effect on the spread rate of wildfires when fuels are dry and the wind is strong. Insight into the processes and variables with strong influence on large-scale fire propagation can only arise from the analysis of wildfire data, rather than experimental fires, field or laboratory, or relying solely on simulation

modelling. Recent research into spot fire controls (Page et al., 2018; Storey et al., 2020a), rate of fire spread in mountain pine beetle-killed stands (Perrakis et al., 2014) and whole fire-atmosphere processes (Dowdy et al., 2017; Brewer and Clements, 2019; McCarthy et al., 2019) are examples of new insights into fire dynamics based on wildfire data that can help us better understand wildfire propagation and guide future fire behaviour modelling efforts.

Advances and deployment of remote sensing technology, better mapping of vegetation and its structure at landscape scales and more accurate measurement of weather variables have created opportunities to reduce the uncertainty associated with the quantification of wildfire propagation for research studies. These data sourcing techniques will in turn lead to improvements of our understanding of fire dynamics, model calibration and more accurate forecasting of wildfire propagation.

On a concluding note, the evaluation of a fire behaviour model or guide constitutes a continuing practice (Watts, 1987). In this regard, we plan to continue to add to the Southern Australian and BONFIRE databases which will allow for the periodic evaluation of the 10% rule of thumb and other fire spread models.

Declaration of competing interest

The authors declare that they have no known competing financial interests or personal relationships that could have appeared to influence the work reported in this paper.

Acknowledgements

PMF and ÂS contribution was carried out in the framework of the UIDB/04033/2020 project, funded by the Portuguese Foundation for Science and Technology (FCT), and the BONFIRE (PTDC/AAG-MAA/2656/2014) project, funded by FCT and the European Regional Development Fund (ERDF) through COMPETE 2020—Operational Program for Competitiveness and Internationalization (POCI). ÂS received support from the Portuguese Foundation for Science and Technology (FCT) through Ph.D. Grant SFRH/BD/132838/2017, funded by the Ministry of Science, Technology and Higher Education, and by the European Social Fund - Operational Program Human Capital within the 2014–2020 EU Strategic Framework.

The authors are indebted to Andrew Sullivan and Matt Plucinski (CSIRO, Australia), Craig Clements and Matthew Brewer (San Jose State University, USA) and Stuart Matthews (NSW RFS, Australia) for their helpful comments on earlier versions of this paper. The assistance of Gavril Xanthopoulos and Miltiadis Athanasiou (Hellenic Agricultural Organization "Demeter", Greece), and Kostas Lagouvardos (National Observatory of Athens, Greece) in the details surrounding the 2018 Mati fire is hereby appreciated.

Appendix

Table A1
Date, fire name, fire run time interval, weather conditions, fuel loads, fire behaviour characteristics, and reliability scores for the Southern Australia wildfire dataset (Harris et al., 2011; Kilinc et al., 2012). The weather data, and in particular U_{10}, should be seen as indicative, not a precise value for the fire run.

Calendar date	Fire name	Fire spread time interval	T (°C)	RH (%)	MC (%)	U_{10} (km h^{-1})	R (km h^{-1})	Fire width (km)	Surface fuel load (kg m^{-2})	Total fuel load (kg m^{-2})	Reliability: weather/ fuel/R[a]
January 16, 1962	Daylesford	21:30–22:30	33	17	4.2	37	1.2	1.6	1.4	2.1	3/3/3
April 4, 1978	Gervasse	16:00–17:30	28	29	5.8	100	8	3.1	0.4	0.4	3/3/3
April 4, 1978	Maranup Ford	11:00–12:00	28	29	5.8	40	5.4	2.0	0.4	0.4	3/3/3
February 16, 1983	Otways	16:00–17:00	41	4	2.5	44	4.5	3.7	1.7	3.0	3/3/4
February 16, 1983	Otways	17:00–18:00	41	5	2.6	44	3.7	5.6	1.6	3.0	3/3/4
February 16, 1983	Otways	18:00–19:30	41	5	2.6	39	5	10.0	1.6	3.0	3/3/4
February 16, 1983	Otways	20:00–21:00	41	5	2.6	47	3.7	11.3	1.1	2.4	3/3/4
February 16, 1983	Cockatoo	20:00–21:05	41	5	2.6	47	0.8	0.4	1.1	1.8	2/3/2
February 16, 1983	Mt Lofty	13:50–15:10	40	10	3.3	41	3.4	1.4	0.7	1.2	3/4/3
January 14, 1985	Anakie	14:40–15:40	42	7	2.9	37	5.9	4.4	0.7	1.1	2/2/2
January 8, 1994	Springwood	13:00–15:30	34	20	4.6	41	3	1.1	2.0	2.7	3/4/5
January 8, 1994	Springwood	16:00–17:30	36	18	4.3	43	2.8	3.3	2.0	2.7	3/4/5
December 2, 1998	Linton	13:00–14:00	28	26	5.5	41	0.8	0.4	1.8	3.0	2/3/2
December 2, 1998	Linton	16:15–18:00	29	23	5.1	30	0.9	1.0	1.7	2.8	2/3/2
March 12, 2006	Riley Road	15:00–17:39	36	9	3.2	33	2.5	1.1	1.7	2.8	3/3/3
December 14, 2006	Coopers Creek	15:00–16:00	35	9	3.2	48	6	2.7	1.8	2.9	3/3/3
December 14, 2006	Coopers Creek	16:00–18:00	27	25	5.4	46	6.1	14.5	1.8	2.9	3/3/3
January 21, 2006	Century Track	16:30–18:30	41	18	4.2	39	4.4	2.8	1.7	2.8	3/3/3
February 7, 2009	Bunyip	13:00–14:00	43	10	3.2	46	4.7	2.0	1.0	2.3	2/3/3
February 7, 2009	Kilmore East	17:00–18:00	41	10	3.2	46	5.8	6.9	1.3	2.4	2/3/3
February 7, 2009	White Timber Spur	13:30–15:00	25	31	6.1	61	1.7	1.1	1.5	1.9	3/3/3
February 7, 2009	White Timber Spur	15:00–16:30	27	26	5.5	55	1.6	1.4	1.4	1.8	3/3/3
February 7, 2009	White Timber Spur	16:30–17:30	27	24	5.2	46	6.7	1.8	1.4	1.8	3/3/3
February 7, 2009	White Timber Spur	17:30–18:30	27	25	5.4	41	5.1	3.1	1.3	1.6	3/3/3
February 7, 2009	White Timber Spur	18:30–19:30	26	26	5.5	52	4.9	3.9	1.2	1.6	3/3/3
February 7, 2009	White Timber Spur	19:30–20:30	25	27	5.6	50	1.9	4.3	1.1	1.5	3/3/3
February 7, 2009	White Timber Spur	20:30–22:00	25	29	5.9	48	1.4	5.2	1.1	1.5	3/3/3
February 6, 2011	Roleystone-Kelmscott	13:30–14:30	23	31	6.2	43	1.7	0.2	1.4	1.8	2/3/5
February 6, 2011	Roleystone-Kelmscott	14:30–15:30	24	29	5.9	39	1.4	0.6	1.4	1.8	2/3/5
February 1, 2011	Tostaree	13:00–16:00	39	13	3.6	31	3.8	1.5	1.9	3.0	3/3/3

[a]See Table A3.

Table A2
Date, fire name and country, vegetation type, weather conditions, rate of fire spread, reliability scores, and fuel loads for the BONFIRE dataset (Fernandes et al., 2020). The weather data, and in particular U_{10}, should be seen as indicative, not a precise value for the fire run.

Calendar date	Fire name, country	Vegetation/ fuel type	T (°C)	RH (%)	MC (%)	U_{10} (km h^{-1})	R (km h^{-1})	Fine fuel load (kg m^{-2})	Reliability: weather/ fuel/R [a]	Source
August 11, 2006	Serra da Ossa, Portugal	Forest - eucalypt	34	15	4.0	37	2.5	15.1	2/2/2	Unpublished data on file with P.M. Fernandes
February 16, 1983	Belgrave, Australia	Forest - eucalypt	42	5	2.6	52	6.6	19.3	2/3/2	Keeves and Douglas (1983)
February 16, 1983	Belgrave, Australia	Forest - eucalypt	41	7	2.9	50	3.5	13.9	2/3/2	Keeves and Douglas (1983)
November 17, 1962	Longford, Australia	Forest - eucalypt	32.7	17	4.3	48	1.4	12.0	1/3/2	McArthur (1965)
November 15, 2002	Redmond, Australia	Forest - eucalypt	35	13	3.5	50	6.0	8.5	2/3/3	McCaw (2003)
February 16, 1983	East Trentham/ Macedon, Australia	Forest - eucalypt	41	5	3.5	44	4.3	24.7	2/3/4	Rawson et al. (1983)
February 16, 1983	East Trentham/ Macedon, Australia	Forest - eucalypt	41	7	3.5	70	11.2	21.6	2/3/4	Rawson et al. (1983)
February 16, 1983	East Trentham/ Macedon, Australia	Forest - eucalypt	41	7	3.5	47	6.0	14.7	2/3/4	Rawson et al. (1983)
February 16, 1983	East Trentham/ Macedon, Australia	Forest - eucalypt	41	7	3.5	33	1.3	22.5	2/3/4	Rawson et al. (1983)
December 20, 1974	Rocky Gully, Australia	Forest - eucalypt	40	10	3.0	70	6.4	15.0	4/3/3	Underwood et al. (1985)
April 4, 1978	Brunswick, Australia	Forest - eucalypt	NA	NA	4.0	52	8.0	NA	3/3/3	Underwood et al. (1985)
February 16, 1983	Deans Marsh, Australia	Forest - eucalypt	40	11	3.0	70	10.0	NA	2/4/3	Rawson et al. (1983)
January 29, 2009	Delburn, Australia	Forest - eucalypt	44.5	10	3.2	42	2.2	15.0	2/3/3	Harris et al. (2011)
February 7, 2009	Maiden Gully, Australia	Forest - eucalypt	44.9	7	2.8	41	1.9	10.0	2/3/3	Harris et al. (2011)
March 8, 1990	Millbrook Road, Australia	Forest - eucalypt	31.5	12	3.7	30	1.5	NA	2/3/3	Pratt (1990)
January 20, 1988	Blackjack, Australia	Forest - eucalypt	29	18	4.4	30	1.5	NA	1/2/1	Bartlett (1993)
January 14, 1962	Dandenongs, Australia	Forest - eucalypt	39.2	12	3.5	39	1.2	13.5	3/3/3	Harris et al. (2011)
January 8, 1969	Maldon, Australia	Forest - eucalypt	37.1	6	2.8	37	0.8	3.0	3/3/3	Harris et al. (2011)
January 13, 1939	Black Friday, Australia	Forest - eucalypt	44.6	9	3.0	56	1.6	16.4	5/3/3	Harris et al. (2011)
January 13, 1939	Colac, Australia	Forest - eucalypt	42.2	9	3.1	56	4.9	13.1	3/3/3	Sullivan (2004)
January 13, 1939	Kyneton, Australia	Forest - eucalypt	42.2	9	3.1	56	5.2	13.9	3/3/3	Sullivan (2004)
January 13, 1939	Tawong, Australia	Forest - eucalypt	46	13	3.5	56	7.9	10.7	3/3/3	Sullivan (2004)
January 18, 2003	Mt Stromlo, Australia	Forest - conifer	37	10	6.0	37	3.5	NA	1/1/1	Gellie (2005)
July 31, 2001	Las Palomas, Spain	Forest - conifer	28	21	4.0	57	2.6	7.4	1/1/1	Rodríguez y Silva and Molina-Martínez (2012)
February 2, 1979	Caroline, Australia	Forest - conifer	37	17	6.0	46	4.8	25.0	2/3/3	Billing (1980)
June 17, 2017	Pedrogão Grande, Portugal	Forest - conifer	31.5	34	7.0	30	2.3	17.3	2/3/2	Guerreiro et al. (2017)
February 26, 1995	Berwick Forest, New Zealand	Forest - conifer	34.5	10	6.0	30	0.5	30.0	1/3/1	Fogarty et al. (1997)
February 26, 1995	Berwick Forest, New Zealand	Forest - conifer	33.5	14	6.0	32	0.9	30.0	1/3/1	Fogarty et al. (1997)
February 26, 1995	Berwick Forest, New Zealand	Forest - conifer	33	16	6.0	33	2.3	30.0	1/3/1	Fogarty et al. (1997)
July 21, 2009	Horta de Sant Joan, Spain	Forest - conifer	38	11	6.0	62	4.9	NA	2/3/1	GRAF (2010)
February 16, 1983	Narraweena, Australia	Forest - conifer	40	10	6.0	80	8.0	NA	2/3/3	Keeves and Douglas (1983)
February 16, 1983	Mount Muirhead, Australia	Forest - conifer	40	10	6.0	80	12.5	NA	2/3/3	Keeves and Douglas (1983)
September 6, 1988	Canyon Creek, USA	Forest - conifer	27	15	6.0	55	6.2	27.9	4/3/2	Goens (1990), Bushey (1991), Ward et al. (1994)
October 20, 1991	East Bay, USA	Forest - conifer	32.2	17	6.0	37	1.5	NA	1/2/1	Alexander (2002), NFPA (1992)
October 15, 2017	Mata Nacional de Leiria, Portugal	Forest - conifer	32.1	19	6.0	37	4.7	13.3	2/2/2	Guerreiro et al. (2018)
August 3, 1936	Galatea Creek, Canada	Forest - conifer	NA	NA	7.0	55	7.8	NA	2/3/1	Fryer and Johnson (1988)
May 8, 1987	Wallace Lake, Canada	Forest - conifer	28	12	6.0	30	3.9	NA	4/3/1	Hirsch (1988)
September 27, 1994	Beerburrum, Australia	Forest - conifer	36.6	12	6.0	50	3.6	NA	1/3/1	Hunt et al. (1995)
November 6, 1994	Beerburrum, Australia	Forest - conifer	24	14	6.0	38	1.6	NA	1/3/1	Hunt et al. (1995)
January 10, 1987	Lago Puelo, Argentina	Forest - conifer	30	20	7.0	30	1.7	NA	4/2/2	Sagarzazu and Defossé (2009)
January 10, 1987	Lago Puelo, Argentina	Forest - conifer	30	20	7.0	50	4.3	NA	4/2/2	Sagarzazu and Defossé (2009)

(*continued on next page*)

Table A2 (*continued*)

Calendar date	Fire name, country	Vegetation/ fuel type	T (°C)	RH (%)	MC (%)	U_{10} (km h^{-1})	R (km h^{-1})	Fine fuel load (kg m^{-2})	Reliability: weather/ fuel/R [a]	Source
July 23, 2018	Mati, Greece	Forest - conifer	38	17	6.0	44	2.6	NA	2/NA/2	Xanthopoulos et al. (2018)
January 10, 1987	Lago Puelo, Argentina	Forest - conifer	30	20	7.0	45	2.3	NA	4/2/2	Sagarzazu and Defossé (2009)
July 27, 2007	Obejo, Spain	Shrubland	39	11	4.5	36	3.1	28.3	1/1/1	Rodríguez y Silva and Molina-Martínez (2012)
July 31, 2001	Sierra Parda, Spain	Shrubland	33	18	5.9	33	4.1	28.3	1/1/1	Rodríguez y Silva and Molina-Martínez (2012)
July 18, 2012	Tavira, Portugal	Shrubland	21	24	6.0	40	2.0	17.0	2/3/2	Viegas et al. (2012)
December 21, 1989	Fitzgerald River NP, Australia	Shrubland	33	12	4.0	42	1.9	NA	2/5/3	McCaw et al. (1992)
December 21, 1989	Fitzgerald River NP, Australia	Shrubland	35	9	3.5	43	3.0	NA	2/5/3	McCaw et al. (1992)
December 21, 1989	Fitzgerald River NP, Australia	Shrubland	35	9	2.0	34	7.5	NA	2/5/3	McCaw et al. (1992)
December 21, 1989	Fitzgerald River NP, Australia	Shrubland	35	9	3.0	43	4.8	NA	2/5/3	McCaw et al. (1992)
July 9, 2013	Picões, Portugal	Shrubland	34	15	5.5	35	4.0	NA	2/3/2	Viegas et al. (2013)
October 15, 2017	Mata Nacional de Leiria, Portugal	Shrubland	29.9	21	4.3	40	6.5	17.1	2/2/2	Guerreiro et al. (2018)
October 15, 2017	Relva Velha, Portugal	Shrubland	32.9	16.8	5.8	35	4.5	15.0	2/3/2	Guerreiro et al. (2018)
September 19, 2010	Machine Gun, USA	Shrubland	32	6	2.9	37	2.6	NA	2/3/1	Frost (2015)
December 22, 1980	Dimboola, Australia	Shrubland	35.7	16	6.1	40	2.0	10.0	3/3/3	Harris et al. (2011)
January 7, 1979	Epuyn Lake, Argentina	Shrubland	30	20	6.6	39	1.1	NA	4/2/2	Sagarzazu and Defossé (2009)
October 9, 2017	Tubbs, USA	Shrubland	32.8	7	4.5	73	6.5	NA	2/3/2	Coen et al. (2018), Nauslar et al. (2018)
August 5, 2018	Perna da Negra, Portugal	Shrubland	24.8	14	6.1	34	2.4	21.7	3/3/3	Rego et al. (2019)

[a]See Table A3.

Table A3
Reliability rating for weather, fuel and fire spread observations for wildfire case studies. Adapted from Cheney et al. (2012) and Cruz et al. (2012).

Rating	Weather	Fuel complex	Rate of spread
1	Nearby (<25 km) meteorological station or direct measurements in the field with high quality instruments, and/or validated modelled wind field.	Fuel characteristics inferred from a fuel age function developed for the particular fuel type and area.	Direct timing of fire spread measurements (i.e. infrared scans, aerial observations, observed reference points with photographs).
2	Meteorological station within 50 km of the fire with no local effects (i.e. terrain, vegetation) on the wind field, and/or partially validated modelled wind field.	Fuel characteristics inferred from a visual assessment or measurements of nearby unburnt forest.	Reliable timing (within ±15 min) of fire spread by field observations with general reference points.
3	Meteorological station within 50 km of the fire but there are local effects on the wind field or the data not representative of the fire area. Meteorological station >50 km of the fire, reconstruction of wind speed for fire site. Unvalidated modelled wind field.	Fuel characteristics inferred from a fuel age curve for a forest type of similar structure.	Reconstruction of fire spread with numerous cross references.
4	Spot meteorological observation near the fire.	Fuel characteristics typical of equilibrium level in the representative fuel type.	Doubtful reconstruction of fire spread.
5	Distant meteorological observations at locations very different to fire site.	Qualitative fuel type description.	Anecdotal or conflicting reports of fire spread.

References

Albini, F.A., 1976. Estimating Wildfire Behavior and Effects. US Department of Agriculture, Forest Service, Intermountain Forest and Range Experiment Station, Ogden, UT. General Technical Report INT-30.

Albini, F.A., Alexander, M.E., Cruz, M.G., 2012. A mathematical model for predicting the maximum potential spotting distance from a crown fire. Int. J. Wildland Fire 21, 609–627.

Alexander, M.E., 2002. An Overview of Systems Used for Rating Fire Danger and Predicting Fire Behavior Used in Canada. In: Lesson 31 Presentation, S-590 Advanced Fire Behavior Interpretation Course. National Advanced Resource Technology Center, Marana, AZ. Mar. 10-22. https://www.frames.gov/catalog/61282.

Alexander, M.E., Cruz, M.G., 2006. Evaluating a model for predicting active crown fire rate of spread using wildfire observations. Can. J. For. Res. 36, 3015–3028.

Anderson, W.R., Cruz, M.G., Fernandes, P.M., McCaw, L., Vega, J.A., Bradstock, R.A., Fogarty, L., Gould, J., McCarthy, G., Marsden-Smedley, J.B., Matthews, S., Mattingley, G., Pearce, H.G., van Wilgen, B.W., 2015. A generic, empirical-based model for predicting rate of fire spread in shrublands. Int. J. Wildland Fire 24, 443–460.

Andrews, P., Finney, M., Fischett, M., 2007. Predicting wildfires. Sci. Am. 297 (2), 47–55.

Andrews, P.L., 2012. Modeling Wind Adjustment Factor and Midflame Wind Speed for Rothermel's Surface Fire Spread Model. US Department of Agriculture, Forest Service, Rocky Mountain Research Station, Fort Collins, CO. General Technical Report RMRS-GTR-266.

Barbero, R., Abatzoglou, J.T., Pimont, F., Ruffault, J., Curt, T., 2020. Attributing increases in fire weather to anthropogenic climate change over France. Front. Earth Sci. 8, 104.

Bartlett, A.G., 1993. A Case Study of Wildfire Management in the Byadbo and Tingaringy Wilderness Areas. Victorian Government, Department of Conservation and Natural Resources, Melbourne, VIC. Fire Management Branch Research Report 38.

Beer, T., Williams, A., 1995. Estimating Australian forest fire danger under conditions of doubled carbon dioxide concentrations. Climatic Change 29, 169–188.

Billing, P.R., 1980. Some Aspects of the Behaviour of the Caroline Fire of February 1979. Forests Commission – Victoria, Division of Forest Protection, Melbourne, VIC. Fire Research Branch Report 7.

Blanchi, R., Leonard, J., Haynes, K., Opie, K., James, M., Oliveira, F.D., 2014. Environmental circumstances surrounding bushfire fatalities in Australia 1901–2011. Environ. Sci. Policy 37, 192–203.

Bowers, C., 2018. The Diablo Winds of Northern California: Climatology and Numerical Simulations (MSc Thesis). San Jose State University, San Jose, CA.
Brewer, M.J., Clements, C.B., 2019. The 2018 Camp Fire: meteorological analysis using in situ observations and numerical simulations. Atmosphere 11, 47.
Bushey, C.L., 1991. Documentation of the Canyon Creek Fire. Volumes 1 and 2, Montana Prescribed Fire Services, Ltd., Billings, MT. US Department of Agriculture, Forest Service. Contract Report #43–03R6–9–360.
Byram, G.M., 1959. Forest fire behavior. In: Davis, K.P. (Ed.), Forest Fire: Control and Use. McGraw-Hill, New York, NY, pp. 90–123.
Catchpole, E.A., Catchpole, W.R., Rothermel, R.C., 1993. Fire behavior experiments in mixed fuel complexes. Int. J. Wildland Fire 3, 45–57.
CFA, 1999. Reducing the Risk of Entrapment in Wildfires – A Case Study of the Linton Fire. Country Fire Authority, Melbourne, VIC.
Cheney, N.P., 1981. Fire Behaviour. In: Gill, A.M., Groves, R.H., Noble, I.R. (Eds.), Fire and the Australian Biota. Australian Academy of Science, Canberra, ACT, pp. 151–175.
Cheney, N.P., Gould, J.S., Catchpole, W.R., 1998. Prediction of fire spread in grasslands. Int. J. Wildland Fire 8, 1–13.
Cheney, N.P., Gould, J.S., McCaw, W.L., Anderson, W.R., 2012. Predicting fire behaviour in dry eucalypt forest in southern Australia. For. Ecol. Manag. 280, 120–131.
Coen, J.L., 2011. Some new basics of fire behavior. Fire Manag. Today 71 (1), 37–42.
Coen, J.L., Schroeder, W., Quayle, B., 2018. The generation and forecast of extreme winds during the origin and progression of the 2017 Tubbs Fire. Atmosphere 9, 462.
Cova, T.J., Dennison, P.E., Kim, T.H., Moritz, M.A., 2005. Setting wildfire evacuation trigger points using fire spread modeling and GIS. Trans. GIS 9, 603–617.
Cruz, M.G., Alexander, M.E., 2013. Uncertainty associated with model predictions of surface and crown fire rates of spread. Environ. Model. Software 47, 16–28.
Cruz, M.G., Alexander, M.E., 2019. The 10% wind speed rule of thumb for estimating a wildfire's forward rate of spread in forests and shrublands. Ann. For. Sci. 76, 44.
Cruz, M.G., Alexander, M.E., Sullivan, A.L., Gould, J.S., Kilinc, M., 2018. Assessing model improvements in predicting wildland fire rates of spread. Environ. Model. Software 105, 54–63.
Cruz, M.G., Alexander, M.E., Wakimoto, R.H., 2005. Development and testing of models for predicting crown fire rate of spread in conifer forest stands. Can. J. For. Res. 35, 1626–1639.
Cruz, M.G., Matthews, S., Gould, J., Ellis, P., Henderson, M., Knight, I., Watters, J., 2010. Fire dynamics in Mallee-Heath: Fuel, Weather and Fire Behaviour Prediction in South Australian Semi-Arid Shrublands. Bushfire Cooperative Research Centre, East Melbourne, VIC. Report A.10.01.
Cruz, M.G., Sullivan, A.L., Gould, J.S., Sims, N.C., Bannister, A.J., Hollis, J.J., Hurley, R. J., 2012. Anatomy of a catastrophic wildfire: the Black Saturday Kilmore East fire in Victoria, Australia. For. Ecol. Manag. 284, 269–285.
Dowdy, A.J., Fromm, M.D., McCarthy, N., 2017. Pyrocumulonimbus lightning and fire ignition on Black Saturday in southeast Australia. J. Geophys. Res. Atmos. 122, 7342–7354.
Fernandes, P.M., 2001. Fire spread prediction in shrub fuels in Portugal. For. Ecol. Manag. 144, 67–74.
Fernandes, P.M., Botelho, H.S., Rego, F.C., Loureiro, C., 2009. Empirical modelling of surface fire behaviour in maritime pine stands. Int. J. Wildland Fire 18, 698–710.
Fernandes, P.M., Sil, Â., Rossa, C.G., Ascoli, D., Cruz, M.G., Alexander, M.E., 2020. Characterizing Fire Behavior Across the Globe. In: Hood, S., Drury, S., Steelman, T., Steffens, R. (Eds.), The Fire Continuum – Preparing for the Future of Wildland Fire: Proceedings of the Fire Continuum Conference, 2018 May 21-24, Missoula, MT. US Department of Agriculture, Forest Service, Rocky Mountain Research Station, Fort Collins, CO, pp. 258–263. Proceedings RMRS-P-78.
Filippi, J.B., Bosseur, F., Mari, C., Lac, C., 2018. Simulation of a large wildfire in a coupled fire-atmosphere model. Atmosphere 9, 218.
Fogarty, L.G., Jackson, A.F., Lindsay, W.T., 1997. Fire Behaviour, Suppression and Lessons from the Berwick Forest Fire of 26 February 1995. New Zealand Forest Research Institute and National Rural Fire Authority, Wellington, NZ, Rotoura. FRI Bulletin 197 Forest and Rural Fire Scientific and Technical Series Report 3.
Frost, S.M., 2015. Fire Environment Analysis at Army Garrison Camp Williams in Relation to Fire Behavior Potential for Gauging Fuel Modification Needs (MSc Thesis). Utah State University, Logan, UT.
Fryer, G.I., Johnson, E.A., 1988. Reconstructing fire behaviour and effects in a subalpine forest. J. Appl. Ecol. 25, 1063–1072.
Gee, A., Anguiano, D., 2020. Fire in Paradise: an American Tragedy. W.W. Norton and Company, New York, NY.
Gellie, N., 2005. Effectiveness of Fire Management Measures in Pine Plantations. Amog Consulting and ECOGIS, Canberra, ACT. Report for Australian Capital Territory (Department of Urban Services).
Giannaros, T.M., Kotroni, V.K., Lagouvardos, K., 2019. IRIS - rapid response fire spread forecasting system: development, calibration and evaluation. Agric. For. Meteorol. 279, 107745.
Goens, D.W., 1990 June 25-29. Meteorological Factors Contributing to the Canyon Creek Blowup, September 6 and 7, 1988. In: Proceedings of Fifth Conference on Mountain Meteorology. American Meteorological Society, Boston, MA, pp. 180–186. Boulder, CO.
Goens, D.W., Andrews, P.L., 1998. Weather and Fire Behavior Factors Related to the Dude Fire, AZ. In: Preprint Volume of Second Symposium on Fire and Forest Meteorology, 1998 Jan. 11-16, Phoenix, AZ. American Meteorological Society, Boston, MA, pp. 153–158.
Goldammer, J.G., Xanthopoulos, G., Dimitrakopoulos, A., Eftychidis, G., Mallinis, G., Mitsopoulos, I., 2019. A year after Greece's wildfire disaster. Crisis Response J. 14 (4), 26–30.
Gould, J.S., McCaw, W.L., Cheney, N.P., Ellis, P.F., Matthews, S., 2007. Field Guide: Fuel Assessment and Fire Behaviour Prediction in Dry Eucalypt Forest, Interim edition. CSIRO Publishing, Collingwood, VIC.
GRAF, 2010. Lo Forestalillo N° 138 20-06-2010. Generalitat de Catalunya, Direcció General de Prevenció, Extinció d'Incendis I Salvaments, Barcelona, Spain ([In Spanish.]).
Guerreiro, J., Fonseca, C., Salgueiro, A., Fernandes, P., Lopez, E., de Neufville, R., Mateus, F., Castellnou, M., Silva, J.S., Moura, J., Rego, F., Mateus, P., 2017. Análise e apuramento dos factos relativos aos incêndios que ocorreram em Pedrógão Grande, Castanheira de Pêra, Ansião, Alvaiázere, Figueiró dos Vinhos, Arganil, Góis, Penela, Pampilhosa da Serra, Oleiros e Sertã entre 17 e 24 de junho de 2017. [Analysis and Fact Finding of the Wildfires Occurring in Pedrógão Grande, Castanheira de Pêra, Ansião, Alvaiázere, Figueiró dos Vinhos, Arganil, Góis, Penela, Pampilhosa da Serra, Oleiros and Sertã Between 17 and 24 June 2017] Comissão Técnica Independente. Assembleia da República. Governo Portugues, Lisboa. Lisboa. Portugal. ([In Portuguese.]). https://www.parlamento.pt/Documents/2017/Outubro/RelatórioCTI_VF%20.pdf.
Guerreiro, J., Fonseca, C., Salgueiro, A., Fernandes, P., Lopez Iglésias, E., de Neufville, R., Mateus, F., Castellnou, R.M., Silva, J.S., Moura, J.M., Rego, F.C., Caldeira, D.N., 2018. Avaliação dos incêndios ocorridos entre 14 e 16 de Outubro de 2017 em Portugal Continental [Study of the Wildfires that Occurred Between 14 and 16 October 2017 in Continental Portugal] Relatório Final. Comissão Técnica Independente. Assembleia da República, Lisboa. Portugal ([In Portuguese.]).
Harris, S., Anderson, W., Kilinc, M., Fogarty, L., 2011. Establishing a Link between the Power of Fire and Community Loss: the First Step towards Developing a Bushfire Severity Scale. Victorian Government, Department of Sustainability and Environment, Melbourne, VIC. Report 89.
Hines, F., Tolhurst, K.G., Wilson, A.A.G., McCarthy, G.J., 2010. Overall Fuel Hazard Assessment Guide, fourth ed. Victorian Government, Department of Sustainability and Environment, Melbourne, VIC. Report 82.
Hirsch, K.G., 1988. An overview of the 1987 Wallace Lake Fire, Manitoba. Fire Manag. Notes 49 (2), 26–27.
Hunt, S., Hamwood, R., Ollerenshaw, S., 1995. Beerburrum Wildfires – September and November 1994. Report by the Wildfire Investigation Committee. Queensland Forest Service, Brisbane, QLD.
Keeves, A., Douglas, D.R., 1983. Forest fires in South Australia on 16 February 1983 and consequent future forest management aims. Aust. For. 46, 148–162.
Kerr, W.L., Buck, C.C., Cline, W.E., Martin, S., Nelson, W.D., 1971. Chapter 9 - fire behavior. In: Nuclear Weapons Effects in a Forest Environment – Thermal and Fire. General Electric Company-TEMPO and Department of Defence Nuclear Information Analysis Center, Santa Barbara, CA, pp. 9-1–9-55. Report N2: TR 2-70.
Kilinc, M., Anderson, W., Price, B., 2012. The Applicability of Bushfire Behaviour Models in Australia. Victorian Government, Department of Sustainability and Environment. DSE Schedule 5: Fire Severity Rating Project, Melbourne, VIC. Technical Report 1.
Koslowsky, R.K., 2019. The Tubbs Fire: the Story of Survival and Recovery. Independently Published, Cloverdale, CA.
Lac, C., Chaboureau, J.P., Masson, V., Pinty, J.P., Tulet, P., Escobar, J., Leriche, M., Barthe, C., Aouizerats, B., Augros, C., Aumond, P., Auguste, F., Bechtold, P., Berthet, S., Bielli, S., Bosseur, F., Caumont, O., Cohard, J.M., Colin, J., Couvreux, F., Cuxart, J., Delautier, G., Dauhut, T., Ducrocq, V., Filippi, J.B., Gazen, D., Geoffroy, O., Gheusi, F., Honnert, R., Lafore, J.P., Lebeaupin Brossier, C., Libois, Q., Lunet, T., Mari, C., Maric, T., Mascart, P., Mogé, M., Molinié, G., Nuissier, O., Pantillon, F., Peyrillé, P., Pergaud, J., Perraud, E., Pianezze, J., Redelsperger, J.L., Ricard, D., Richard, E., Riette, S., Rodier, Q., Schoetter, R., Seyfried, L., Stein, J., Suhre, K., Taufour, M., Thouron, O., Turner, S., Verrelle, A., Vié, B., Visentin, F., Vionnet, V., Wautelet, P., 2018. Overview of the meso-NH model version 5.4 and its applications. Geosci. Model Dev. (GMD) 11, 1929–1969.
Lagouvardos, K., Kotroni, V., Bezes, A., Koletsis, I., Kopania, T., Lykoudis, S., Mazarakis, N., Papagiannaki, K., Vougioukas, S., 2017. The automatic weather stations NOANN network of the National Observatory of Athens: operation and database. Geosci. Data J. 4, 4–16.
Lagouvardos, K., Kotroni, V., Giannaros, T.M., Dafis, S., 2019. Meteorological conditions conducive to the rapid spread of the deadly wildfire in Eastern Attica, Greece. Bull. Am. Meteorol. Soc. 100, 2137–2145.
Li, D., Cova, T.J., Dennison, P.E., 2019. Setting wildfire evacuation triggers by coupling fire and traffic simulation models: a spatiotemporal GIS approach. Fire Technol. 55, 617–642.
Luke, R.H., McArthur, A.G., 1978. Bushfires in Australia. Australian Government Publishing Service, Canberra, ACT.
Matthews, S., Gould, J.S., McCaw, L., 2010. Simple models for predicting dead fuel moisture in eucalyptus forests. Int. J. Wildland Fire 19, 1–9.
McArthur, A.G., 1965. Fire Behaviour Characteristics of the Longford Fire. Commonwealth of Australia. Forest and Timber Bureau, Canberra, ACT. Leaflet 91.
McArthur, A.G., 1967. Fire Behaviour in Eucalypt Forests. Commonwealth of Australia, Forestry and Timber Bureau, Canberra, ACT. Leaflet 107.
McCarthy, N., McGowan, H., Guyot, A., Dowdy, A., 2018. Mobile Xpol radar: a new tool for investigating pyroconvection and associated wildfire meteorology. Bull. Am. Meteorol. Soc. 99, 1177–1195.
McCarthy, N., Guyot, A., Dowdy, A., McGowan, H., 2019. Wildfire and weather radar: a review. J. Geophys. Res. Atmos. 124, 266–286.
McCaw, W.L., 2003. Report of an Investigation into the Origin of Bushfires on 15 November 2002 in the Sheepwash and Redmond Areas Adjoining the Hay River, South-Western Australia. Western Australia Department of Conservation and Land Management, Perth, WA (Unpublished Report).

McCaw, L., Maher, T., Gillen, K., 1992. Wildfires in the Fitzgerald River, National Park, Western Australia, December 1989. Western Australia Department of Conservation and Land Management, Perth, WA. Technical Report 26.
Monedero, S., Ramirez, J., Cardil, A., 2019. Predicting fire spread and behaviour on the fireline. Wildfire analyst pocket: a mobile app for wildland fire prediction. Ecol. Model. 392, 103–107.
Nauslar, N.J., Abatzoglou, J.T., Marsh, P.T., 2018. The 2017 North Bay and Southern California fires: a case study. Fire 1, 18.
Neale, T., May, D., 2018. Bushfire simulators and analysis in Australia: insights into an emerging sociotechnical practice. Environ. Hazards 17, 200–218.
Neale, T., May, D., 2020. Fuzzy boundaries: simulation and expertise in bushfire prediction. Soc. Stud. Sci. 50 (in press). https://journals.sagepub.com/doi/abs/10.1177/0306312720906869?journalCode=sssb.
Nelson Jr., R.M., 2001. Water relations of forest fuels. In: Johnson, E.A., Miyanishi, K. (Eds.), Forest Fires: Behavior and Ecological Effects. Academic Press, San Diego, CA, pp. 79–149.
NFPA, 1992. Oakland/Berkeley Hills Fire. National Fire Protection Association, Quincy, MA.
Page, W.G., Wagenbrenner, N.S., Butler, B.W., Blunck, D.L., 2018. An analysis of spotting distances during the 2017 fire season in the Northern Rockies, USA. Can. J. For. Res. 49, 317–325.
Perrakis, D.D.B., Lanoville, R.A., Taylor, S.W., Hicks, D., 2014. Modeling wildfire spread in mountain beetle-affected forest stands, British Columbia, Canada. Fire Ecol 10 (2), 10–35.
Plucinski, M.P., 2019a. Fighting flames and forging firelines: wildfire suppression effectiveness at the fire edge. Curr. For. Rep. 5, 1–19.
Plucinski, M.P., 2019b. Contain and control: wildfire suppression effectiveness at incidents and across landscapes. Curr. For. Rep. 5, 20–40.
Plucinski, M.P., Sullivan, A.L., Rucinski, C.J., Prakash, M., 2017. Improving the reliability and utility of operational bushfire behaviour predictions in Australian vegetation. Environ. Model. Software 91, 1–12.
Potter, B.E., 2002. A dynamics based view of atmosphere–fire interactions. Int. J. Wildland Fire 11, 247–255.
Potter, B.E., 2005. The role of released moisture in the atmospheric dynamics associated with wildland fires. Int. J. Wildland Fire 14, 77–84.
Pratt, J., 1990. The Millbrook Fire, March 8 1990. Woods and Forests Department of South Australia, Adelaide, SA (Unpublished Report).
R Core Team, 2019. R: A Language and Environment for Statistical Computing. R Foundation for Statistical Computing, Vienna, Austria.
Ramirez, J., Monedero, S., Silva, C.A., Cardil, A., 2019. Stochastic decision trigger modelling to assess the probability of wildland fire impact. Sci. Total Environ. 694, 133505.
Rawson, R.P., Billing, P.R., Duncan, S.F., 1983. The 1982-83 forest fires in Victoria. Aust. For. 46, 163–172.
Rego, F., Fernandes, P., Silva, J.S., Azevedo, J., Moura, J.M., Oliveira, E., Cortes, R., Viegas, D.X., Caldeira, D., Santos, F.D., 2019. Relatório de Avaliação do Incêndio de Monchique. [Evaluation Report on the Monchique Wildfire] Observatório Técnico Independente. Assembleia da República, Lisboa, Portugal ([In Portuguese.]). https://www.parlamento.pt/Documents/2019/maio/FINAL-Relatorio-Monchique.pdf.
Rodríguez y Silva, F., Molina-Martínez, J., 2012. Modeling Mediterranean forest fuels by integrating field data and mapping tools. Eur. J. For. Res. 131, 571–582.
Rothermel, R.C., 1983. How to Predict the Spread and Intensity of Forest and Range Fires. US Department of Agriculture, Forest Service, Intermountain Forest and Range Experiment Station, Ogden, UT. General Technical Report INT-143.
Rothermel, R.C., 1991. Predicting Behavior and Size of Crown Fires in the Northern Rocky Mountains. US Department of Agriculture, Forest Service, Intermountain Research Station, Ogden, UT. Research Paper INT-438.
Ryan, K.C., 1991. Vegetation and wildland fire: implications of global climate change. Environ. Int. 17, 169–178.
Sagarzazu, A.M.S., Defossé, G.E., 2009. Study of a 2nd set of largest past fires. European Commission, Brussels, Belgium. Deliverable D8.3-1 of the integrated project "Fire Paradox". Project FP6-018505. http://www.eufirelab.org/toolbox2/library/upload/2830.pdf.
Scott, A.C., Bowman, D.M.J.S., Bond, W.J., Pyne, S.J., Alexander, M.E., 2014. Fire on Earth: an Introduction. John Wiley & Sons, Ltd., Chichester, UK.
Smith, C., Hatchett, B.J., Kaplan, M., 2018. A surface observation based climatology of diablo-like winds in California's wine country and western Sierra Nevada. Fire 1, 25.
Storey, M.A., Price, O.F., Bradstock, R.A., Sharples, J.J., 2020b. Analysis of variation in distance, number, and distribution of spotting in southeast Australian wildfires. Fire 3, 10.
Storey, M.A., Price, O.F., Sharples, J.J., Bradstock, R.A., 2020a. Drivers of long-distance spotting during wildfires in south-eastern Australia. Int. J. Wildland Fire 29, 459–472.
Sullivan, A., 2004. Nature of Severe Fire Events. CSIRO Forestry and Forest Products, Canberra, ACT. Client Report 1470.
Taylor, S.W., Alexander, M.E., 2018. A Field Guide to the Canadian Forest Fire Behavior Prediction (FBP) System, Third ed. Natural Resources Canada, Canadian Forest Service, Northern Forestry Centre, Edmonton, AB. Special Report 11.
Teague, B., McLeod, R., Pascoe, S., 2010. 2009 Victorian Bushfires Royal Commission: Final Report Summary. Government Printer for the State of Victoria, Melbourne, VIC.
Tedim, F., Leone, V., McGee, T.K. (Eds.), 2020. Extreme Wildfire Events and Disasters: Root Causes and New Management Strategies. Elsevier Inc., Amsterdam, Netherlands.
Tennekes, H., 1973. The logarithmic wind profile. J. Atmos. Sci. 30, 234–238.
Underwood, R.J., Sneeuwjagt, R.J., Styles, H.G., 1985. The Contribution of Prescribed Burning to Forest Fire Control in Western Australia: Case Studies. In: Ford, J.R. (Ed.), Proceedings of the Symposium on Fire Ecology and Management in Western Australian Ecosystems, 1985 May 10-11. Perth, WA. Western Australia Institute of Technology, Perth, WA, pp. 153–170.
Viegas, D.X., Figueiredo, A.R., Almeida, A.M., Reva, V., Ribeiro, L.M., Viegas, M.T., Oliveira, R., Raposo, J.R., 2012. Relatório do incêndio florestal de Tavira/São Brás de Alportel [Report on the Tavira/São Brás de Alportel Wildfire] Centro de Estudos sobre Incêndios Florestais, Universidade de Coimbra, ADAI/LAETA, Coimbra, Portugal. ([In Portuguese.]) Available at: http://www.portugal.gov.pt/media/730414/rel_incendio_florestal_tavira_jul2012.pdf.
Viegas, D.X., Ribeiro, L.M., Almeida, M.A., Oliveira, R., Viegas, M.T.P., Reva, V., 2013. Os grandes incêndios florestais e os acidentes mortais ocorridos em 2013. [The Large Wildfires and Fatal Incidents Occurring in 2013. Universidade de Coimbra, ADAI/LAETA, Coimbra, Portugal ([In Portuguese.]).
Wagenbrenner, N.S., Forthofer, J.M., Lamb, B.K., Shannon, K.S., Butler, B.W., 2016. Downscaling surface wind predictions from numerical weather prediction models in complex terrain with WindNinja. Atmos. Chem. Phys. 16, 5229–5241.
Walker, J., 1981. Fuel Dynamics in Australian Vegetation. In: Gill, A.M., Groves, R.H., Noble, I.R. (Eds.), Fire and the Australian Biota. Australian Academy of Science, Canberra, ACT, pp. 101–127.
Ward, D.E., Rothermel, R.C., Bushey, C.L., 1994. Particulate Matter and Trace Gas Emissions from the Canyon Creek Fire of 1988. In: Proceedings of the 12th Conference on Fire and Forest Meteorology, 1993 Oct 26-28, Jekyll Island, GA. Society of American Foresters, Bethesda, MD. SAF Publication 94-02. pp. 62–76.
Watkins, D., Griggs, T., Lee, J.C., Park, H., Singhvi, A., Wallace, T., Ward, J., 2017. How California's most destructive wildfire spread, hour by hour. The New York Times. https://www.nytimes.com/interactive/2017/10/21/us/california-fire-damage-map.html.
Watts Jr., J.M., 1987. Validating fire models. Fire Technol. 23, 93–94.
Willmott, C.J., 1982. Some comments on the evaluation of model performance. Bull. Am. Meteorol. Soc. 63, 1309–1313.
Xanthopoulos, G., Athanasiou, M., 2019. A tale of two fires and a seaside tragedy. Wildfire 28 (2), 18–21.
Xanthopoulos, G., Athanasiou, M., Kaoukis, K., 2018. Η τραγωδία της 23ης Ιουλίου 2018 στην Ανατολική Αττική και τα διδάγματά της [The Tragedy of 23-7-2018 in eastern Attica. Demeter vol. 23, 4–7 ([In Greek.]).